

Dendritic cell vaccines targeting tumor blood vessel antigens in combination with dasatinib induce therapeutic immune responses in patients with checkpoint-refractory advanced melanoma

Walter J Storkus ¹, Deena Maurer,² Yan Lin,³ Fei Ding,⁴ Anamika Bose,⁵ Devin Lowe,⁶ Amy Rose,⁷ Melissa DeMark,⁸ Lilit Karapetyan,⁹ Jennifer L Taylor,¹ Manoj Chelvanambi,¹⁰ Ronald J Fecek,¹¹ Jessica N Filderman,¹⁰ Timothy J Looney,¹² Lauren Miller,¹³ Elizabeth Linch,¹³ Geoffrey M Lowman ¹³, Pawel Kalinski,¹⁴ Lisa H Butterfield ^{15,16}, Ahmad Tarhini ¹⁷, Hussein Tawbi ¹⁸, John M Kirkwood¹⁹

To cite: Storkus WJ, Maurer D, Lin Y, *et al.* Dendritic cell vaccines targeting tumor blood vessel antigens in combination with dasatinib induce therapeutic immune responses in patients with checkpoint-refractory advanced melanoma. *Journal for ImmunoTherapy of Cancer* 2021;9:e003675. doi:10.1136/jitc-2021-003675

► Additional supplemental material is published online only. To view, please visit the journal online (<http://dx.doi.org/10.1136/jitc-2021-003675>).

WJS and DM are joint first authors.

HT and JMK are joint senior authors.

Accepted 17 October 2021



© Author(s) (or their employer(s)) 2021. Re-use permitted under CC BY-NC. No commercial re-use. See rights and permissions. Published by BMJ.

For numbered affiliations see end of article.

Correspondence to

Professor Walter J Storkus; storkuswj@upmc.edu

ABSTRACT

Background A first-in-human, randomized pilot phase II clinical trial combining vaccines targeting overexpressed, non-mutated tumor blood vessel antigens (TBVA) and tyrosine kinase inhibitor dasatinib was conducted in human leukocyte antigen (HLA)-A2⁺ patients with advanced melanoma.

Methods Patient monocyte-derived type-1-polarized dendritic cells were loaded with HLA-A2-presented peptides derived from TBVA (DLK1, EphA2, HBB, NRP1, RGS5, TEM1) and injected intradermally as a vaccine into the upper extremities every other week. Patients were randomized into one of two treatment arms receiving oral dasatinib (70 mg two times per day) beginning in week 5 (Arm A) or in week 1 (Arm B). Trial endpoints included T cell response to vaccine peptides (interferon- γ enzyme-linked immunosorbent spot), objective clinical response (Response Evaluation Criteria in Solid Tumors V.1.1) and exploratory tumor, blood and serum profiling of immune-associated genes/proteins.

Results Sixteen patients with advanced-stage cutaneous (n=10), mucosal (n=1) or uveal (n=5) melanoma were accrued, 15 of whom had previously progressed on programmed cell death protein 1 (PD-1) blockade. Of 13 evaluable patients, 6 patients developed specific peripheral blood T cell responses against ≥ 3 vaccine-associated peptides, with further evidence of epitope spreading. All six patients with specific CD8⁺ T cell response to vaccine-targeted antigens exhibited evidence of T cell receptor (TCR) convergence in association with preferred clinical outcomes (four partial response and two stabilization of disease (SD)). Seven patients failed to respond to vaccination (one SD and six progressive disease). Patients in Arm B (immediate dasatinib) outperformed those in Arm A (delayed dasatinib) for immune response rate (IRR; 66.7% vs 28.6%), objective response rate (ORR) (66.7%

vs 0%), overall survival (median 15.45 vs 3.47 months; p=0.0086) and progression-free survival (median 7.87 vs 1.97 months; p=0.063). IRR (80% vs 25%) and ORR (60% vs 12.5%) was greater for females versus male patients. Tumors in patients exhibiting response to treatment displayed (1) evidence of innate and adaptive immune-mediated inflammation and TCR convergence at baseline, (2) on-treatment transcriptional changes associated with reduced hypoxia/acidosis/glycolysis, and (3) increased inflammatory immune cell infiltration and tertiary lymphoid structure neogenesis.

Conclusions Combined vaccination against TBVA plus dasatinib was safe and resulted in coordinating immunologic and/or objective clinical responses in 6/13 (46%) evaluable patients with melanoma, particularly those initiating treatment with both agents.

Trial registration number NCT01876212.

INTRODUCTION

The incidence of melanoma continues to rise, with American Cancer Society estimates of >100,000 diagnoses of this form of cancer in 2021, and over 7180 disease-associated deaths.¹ The landscape of first-line treatment options for patients with advanced-stage IIIB-IV melanoma has been recalibrated over the past decade with the advent of targeted small molecule inhibitors (ie, BRAFi, MEKi) and immune checkpoint blockade, resulting in increased rates of objective clinical response (OCR) but also a significant rise in the incidence of immune-related adverse events.^{2,3} Despite improved rates of response, most patients with melanoma exhibit primary

or acquired resistance to immune checkpoint blockade, reinforcing the need to develop effective salvage therapies.⁴

Although melanoma vaccines have been universally well-tolerated by patients,⁵ their performance in past phase II/III trials has proven disappointing overall, with minimal clinical benefits reported versus new standard-of-care therapies.⁶ Numerous factors have been posited to limit vaccine efficacy in patients with cancer, including variance in host immune competency, heterogeneity in tumor antigenicity/immunogenicity, a tumor micro-environment (TME) refractory to vaccine-induced T effector cell infiltration and sustained ‘fitness’, and expansion of immunoregulatory networks, among others.^{3 5 7} We have previously demonstrated in preclinical models that vaccines targeting non-mutated antigens (ie, DLK1, EphA2, HBB, NRP1, RGS5 and TEM1) overexpressed by tumor-associated (but not normal tissue-associated) vascular endothelial cells or pericytes promote T cell-dependent tumor vascular normalization in mice, resulting in superior immune cell recruitment, a pro-inflammatory TME and slowed tumor growth or regression.^{8–10} While dasatinib monotherapy is ineffective in treating patients with advanced melanoma,¹¹ we and others have also reported that dasatinib functions as a potent adjuvant to specific vaccination in murine melanoma models.^{12 13} In this context, the combination of dasatinib +vaccine therapy promoted: (1) superior expansion and recruitment of therapeutic T cells into tumors (via locoregional production of CXCR3 ligand chemokines), (2) reduced tumor hypoxia and prevalence of myeloid-derived suppressor cells (MDSC) and regulatory T cells (Treg), (3) broadening/spreading in the anti-tumor CD8⁺ T cell repertoire, and (4) extended overall survival.¹²

Based on these translational findings, we developed a single-center, prospective randomized pilot phase II clinical trial combining these modalities for the treatment of human leukocyte antigen (HLA)-A2⁺ patients with advanced melanoma. We confirmed the safety, immunogenicity and antitumor efficacy of intradermal administration of autologous type-1 dendritic cells (α DC1) loaded with a mixture of six HLA-A2-presented peptides derived from the tumor-associated vascular antigens DLK1, EphA2, HBB, NRP1, RGS5 and TEM1 combined with daily oral administration of dasatinib (70 mg two times per day) as an immune adjuvant/conditioning agent in patients who had failed prior therapies, including checkpoint blockade.

MATERIALS AND METHODS

Patients

This was a single-center, first-in-human, prospective randomized pilot phase II clinical trial (University of Pittsburgh Cancer Institute (UPCI) 12-048) for HLA-A2⁺ patients with advanced-stage (IIC-IV) cutaneous, mucosal or uveal melanoma (performed between May 2014

and July 2019) for whom standard curative or palliative measures did not exist or were no longer effective. The study was ended due to conclusion of NIH R01 CA169118 grant support. Patient eligibility/exclusion criteria are described in online supplemental materials. Informed consent was obtained from all patients entered onto this study. Patient demographic information is provided in online supplemental table S1.

Autologous α DC1/TBVA peptide vaccine generation (BB-IND 15224)

Patient α DC1 vaccines were generated from apheresis products and quality controlled as previously described,¹⁴ with further details provided in online supplemental file 3. Aliquots of cryopreserved vaccine α DC1 were analyzed for transcriptional and proteomic profiles in exploratory studies using Affymetrix GeneChips and FACS analysis, respectively, as described below (online supplemental figure 1).

Study design and treatment

Sixteen patients were enrolled, with one patient voluntarily withdrawing from trial prior to vaccine generation and one patient expiring after vaccine generation but prior to treatment. Of the 14 patients receiving treatment, 13 were evaluable for all endpoint analyses, with 1 patient expiring prior to the completion of treatment cycle 1. Patients were randomized onto one of two treatment arms (figure 1A). All treated patients received an autologous α DC1/peptide vaccine administered by a single intradermal injection of approximately 10⁷ cells on days 1 and 15 of each monthly therapy cycle. Intradermal administration of the vaccine was provided in the vicinity of the nodal drainage groups of the four extremities and was performed on an outpatient basis in the Hillman Cancer Center Clinical and Translational Research Center. Patients on Arm A started dasatinib administration (70 mg orally two times per day) on cycle 2, day 1 (ie, in week 5), while patients on Arm B began dasatinib administration on cycle 1, day 1 (ie, in week 1). Study treatment was continued for at least six cycles or until disease progression, intercurrent illness preventing further treatment, unacceptable adverse event(s), or unacceptable changes in the patient’s condition. Patients were followed for 1 year after removal from study treatment or until death, whichever occurred first.

Study endpoints

The primary endpoint of this clinical trial was patient peripheral blood T cell response to vaccine peptides based on interferon (IFN)- γ enzyme-linked immunosorbent spot (ELISPOT) analyses. Secondary endpoints included safety and investigator-assessed OCR and objective response rate (ORR) by Response Evaluation Criteria in Solid Tumors (RECIST) V.1.1, progression-free survival (PFS), overall survival (OS) and exploratory analyses of patient blood, tumor and serum specimens for treatment-associated changes in Treg/MDSC content (blood),

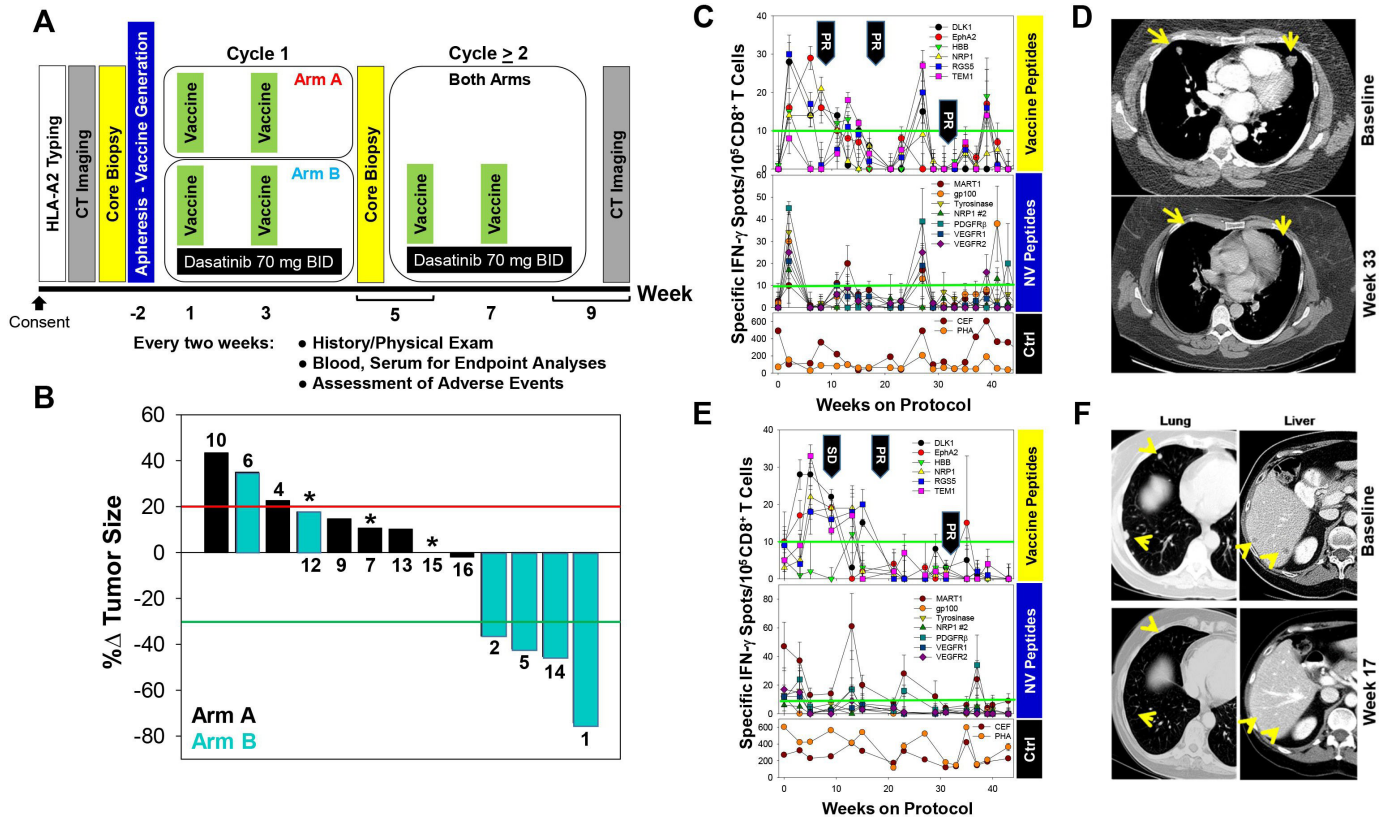


Figure 1 Protocol schema and examples of immunologic and clinical responses to treatment with dendritic cell/tumor blood vessel antigens peptide-based vaccines + dasatinib. In (A), outline of treatment schema on Arm A (vaccine + dasatinib beginning in week 5) or Arm B (vaccine + dasatinib beginning in week 1). In (B), a waterfall plot is provided depicting greatest change in tumor burden on-treatment, with 20% increase/30% decrease in tumor size indicated by solid red/green horizontal lines, respectively. Inset numbers reflect patient #. *Patients with progressive disease based on development/progression of new disease sites on-treatment. Patients #1 (B/D) and #5 (panels E/F) were both treated on Arm B of this trial and developed coordinate immune response to vaccine peptides as well as non-vaccine, but disease-relevant peptides as determined in IFN- γ enzyme-linked immunosorbent spot assays (C/E), and objective partial clinical responses exemplified by shrinkage of visceral metastases in positron emission tomography/CT imaging (D/F). Yellow arrows in panels D and F indicate target lesions at baseline versus on-treatment. BID, two times per day; Ctrl, control stimuli (peptides derived from cytomegalovirus, Epstein-Barr virus and influenza virus (CEF) proteins; HLA, human leukocyte antigen; IFN, interferon; NV, non-vaccine; PR, partial response; SD, stabilization of disease.

vascular structure (tumor) and pro-inflammatory CXCL10 levels (serum). Radiographic imaging was performed at baseline and then approximately every 8–9 weeks until disease progression by CT or positron emission tomography/CT. Response assessments were predicated on RECIST V.1.1 criteria. Adverse events (AEs) were evaluated using the National Cancer Institute Common Terminology Criteria for Adverse Events V.4.0. Tumor biopsies were obtained prior to treatment and at week 5 on-treatment. Peripheral blood specimens were obtained at baseline and then every 2 weeks while on the study protocol. Biopsy tissues were analyzed using quantitative real-time PCR (qRT-PCR) and Thermo Fisher Ion Torrent-based transcriptional profiling platforms (Oncomine TCRB-LR Assay, Oncomine Immune Response Research Assay (OIRRA)).

IFN γ ELISPOT assays

Patient peripheral blood T cell responses against peptides in the vaccine formulation were examined

using standardized IFN γ ELISPOT assays as previously described,¹⁵ with further details provided in online supplemental materials. A positive ELISPOT finding on-treatment was defined as a greater than twofold increase in spot-forming reactive T cells versus baseline and at least 10 specific spots (minus background for T2 cells only) per 10^5 immune cells plated. Primary endpoint was considered positive if the patient responded positively against three or more peptides in the vaccine formulation at any time point on-treatment.

Flow cytometry

Baseline and on-treatment patient peripheral blood mononuclear cells were analyzed for frequencies of CD4⁺Foxp3⁺ Treg, HLA-DR^{neg}CD3^{neg}CD11b⁺CD14⁺CD15^{neg}CD19^{neg}CD33⁺ monocytic MDSC (M-MDSC) and HLA-DR^{neg}CD3^{neg}CD11b⁺CD14^{neg}CD15⁺CD19^{neg}CD33⁺ polymorphonuclear MDSC (PMN-MDSC) using an LSRFortessa flow cytometer (BD Biosciences, San Jose,

California, USA) within the Department of Immunology's Unified Flow Core. Vaccine dendritic cells were also phenotyped for expression of costimulatory or check-point molecules by flow cytometry as detailed in online supplemental methods.

RNA isolation and gene expression analyses

Total RNA was isolated from vaccine α DC1, tumor biopsies and peripheral blood mononuclear cells and subjected to qRT-PCR and GeneChip Human Genome U133A 2.0 Arrays (Thermo Fisher Scientific) profiling performed by the University of Pittsburgh Genomics Research Core, to the Oncomine TCRB-LR Assay and to the Oncomine Immune Response Research Assay (OIRRA; Thermo Fisher Scientific, Carlsbad, California, USA) under an institutional material transfer agreement. TCR β chain repertoire libraries were constructed by multiplex PCR utilizing FR1 and constant gene targeting primers via the Oncomine TCRB-LR assay, then sequenced using the Ion Torrent S5 to a target depth of 1.5M raw reads per library. To evaluate T cell receptor (TCR) convergence, we searched for instances where TCR β chains were identical in amino acid space but had distinct nucleotide sequences owing to N-addition and exonucleotide chewback within the V-D and D-J junctions of the complementary determining region 3. Targeted gene expression profiling of pretreatment and post-treatment tumor biopsies was performed using the OIRRA and total RNA input.

Biostatistics and bioinformatics analyses

Details for biostatistical and bioinformatic methods may be found in online supplemental file 3.

RESULTS

Autologous α DC1/TBVA peptide vaccines + dasatinib are safe, immunogenic and promote clinical responses in PD-1-resistant patients with melanoma in association with extended OS

Fourteen of 16 patients received autologous α DC1/tumor blood vessel antigens (TBVA) peptide vaccines plus dasatinib in two treatment arms distinguished by the start date for dasatinib administration (figure 1, online supplemental figure S1A). The treatment arms were chosen to allow for a comparison of immunogenicity induced by vaccine alone versus vaccine + dasatinib in the first cycle, and to test whether concurrent or sequential administration of dasatinib is more effective. Thirteen of these 14 patients were evaluable for endpoint blood, serum and tumor biopsy analyses at the week 5 time point and CT imaging beginning in week 8/9, with 1 patient expiring in association with disease progression prior to completing cycle 1 of treatment. Although patient immunologic response to vaccine peptides was the primary endpoint in this study, we were struck by unexpected reductions in patient tumor sizes on-treatment, particularly for individuals treated on Arm B versus Arm A (figure 1B; $p=0.044$). Of the 13 evaluable patients, 6 patients (2 in Arm A and

4 in Arm B) developed specific peripheral blood CD8⁺ T cell responses against ≥ 3 of the vaccine peptides that were not detected at baseline based on results obtained in IFN- γ ELISPOT assays (figures 1 and 2). As depicted in figure 1C (patient #1, Arm B) and figure 1E (patient #5, Arm B) examples, vaccine-specific immune responses were detectable as early as trial week 3, with undulating levels of peptide-specific CD8⁺ T cells observed in longitudinal monitoring of peripheral blood on-treatment. Each of the six vaccine peptides was recognized by at least three evaluable patients, with peptides DLK1₃₁₀₋₃₁₈, EphA2₈₈₃₋₈₉₁, HBB₃₁₋₃₉, NRPI₄₃₃₋₄₄₁, RGS5₅₋₁₃ and TEM1₆₉₁₋₇₀₀ recognized by 6/6, 3/6, 5/6, 5/6, 4/6 and 4/6 of the immunologic responder patients on-treatment, respectively (figure 2A).

Notably, four out of six patients exhibiting vaccine-specific T cell responses developed OCRs (four partial response (PR) and two stabilization of disease (SD); figure 1D,F and 2A), and of the seven patients that failed to respond immunologically to vaccination, one patient exhibited SD (PFS, OS=8.3 months) while six patients had progressive disease (PD). Of the four patients achieving a PR on this trial, on-treatment CD8⁺ T cell responses were detected against the vaccine DLK1, EphA2, HBB, NRPI, RGS5 and TEM1 peptides in 4/4, 2/4, 4/4, 3/4, 2/4 and 3/4 cases, respectively (figure 2A). Patients treated on Arm B (ie, combined vaccine + immediate dasatinib from treatment outset) displayed significantly improved OS (median 19.1 vs 8.3 months; $p=0.0086$) and a trend for improved PFS (median 7.9 vs 2.2 months; $p=0.063$) versus patients treated on Arm A (ie, vaccine + delayed dasatinib administration beginning in week 5; figure 2B, online supplemental table S2). Patient T cell response to vaccine peptides (figure 2C) and non-vaccine (NV; ie, 'spread') peptides (figure 2D) as determined in IFN- γ ELISPOT assays was predictive of extended OS in vaccinated patients.

Overall, the combination vaccine + dasatinib immunotherapy was well-tolerated, with no treatment-related AEs > grade 3 observed (online supplemental tables S3 and S4). Among the 15 patients receiving at least one vaccine, the most commonly observed AEs included anemia (8 patients), fatigue (10 patients) and hyponatremia (9 patients), consistent with AEs reported for dasatinib monotherapy. Patients treated on Arm B versus Arm A had increased incidence of fever (33% vs 0%), headache (33% vs 0%), maculopapular rash (50% vs 11%), nausea (83% vs 11%), neutrophil count reduction (67% vs 22%), platelet count reduction (50% vs 22%) and vomiting (67% vs 0%).

Clinical benefit of vaccination is associated with epitope spreading in patient T cell response against non-vaccine tumor and vascular antigens, and with increased TCR convergence

Given previous reports for epitope/determinant spreading in vaccinated patients with melanoma with superior outcomes in immunotherapy trials,¹⁶ and the ability of dasatinib to improve epitope spreading when

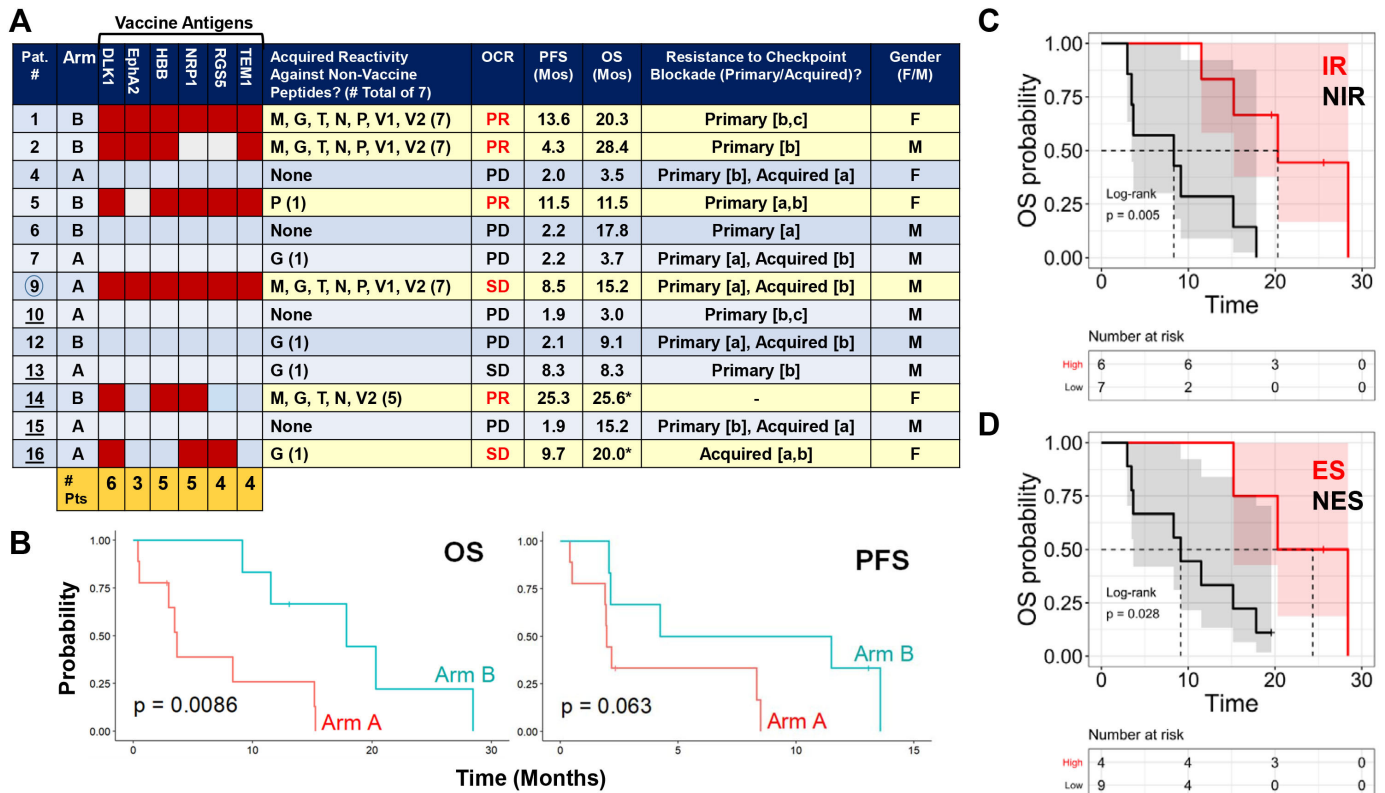


Figure 2 Summary of immunologic and clinical response data. In (A), a summary is provided for individual patient treatment arm, response to individual TBVA peptides used in the vaccine and spread (non-vaccine) peptides derived from TBVA or melanoma-associated antigens (interferon- γ enzyme-linked immunosorbent spot), OCR, PFS, OS, prior primary or acquired resistance to treatment with checkpoint blockade, and gender. For resistance to checkpoint blockade status, prior treatments included anti-CTLA4 [a], anti-PD-1 [b] and combined anti-CTLA4 + anti-PD-1 [c]. Pt. # (underlined) indicates patients with uveal melanoma. Circled Pt. # indicates a patient with mucosal melanoma. *indicates patient still alive. In (B), Kaplan-Meier plots comparing treatment arm versus patient OS and PFS are depicted. Patient immune response to vaccine peptides versus epitope spreading in the response to non-vaccine peptides is correlated to patient OS in panels (C and D), respectively. CTLA-4, cytotoxic T lymphocyte-associated antigen-4; ES, epitope spreading; IR, immune response to vaccine peptides; Mos, Months; NES, no epitope spreading; NIR, no immune response to vaccine peptides; OCR, objective clinical response; OS, overall survival; PD, progressive disease; PFS, progression-free survival; PR, partial response; Pt. patient; SD, stabilization of disease; TBVA, tumor blood vessel antigens.

combined with DC/peptide-based vaccination in murine melanoma models,¹² we investigated on-treatment patient peripheral blood CD8⁺ T cell reactivity against HLA-A2-presented, vaccine-unrelated peptide epitopes (ie, NV peptides) derived from melanoma antigens (MART-1, gp100, tyrosinase) or TBVA (NRP1, PDGFR β , VEGFR1, VEGFR2) using IFN- γ ELISPOT assays (figure 1C,E and 2A). As exemplified for patients #1 and #5 (both PR, Arm B) in figure 1C,E, spread T cell responses were detected in patient peripheral blood on-treatment largely in a temporally coordinate manner with (or slightly delayed from) specific T cell responses against vaccine peptide epitopes, with spread responses against > 2 of the seven screened NV peptides only detected in patients #1 (PR), #2 (PR), #9 (SD) and #14 (PR) (figure 2A). The number of vaccine peptides recognized by patient peripheral blood T cells on-treatment was correlated with the number of NV peptides recognized by that same individual ($p=0.0019$; online supplemental figure S2). When considering T cell responses based on the total number of

peptide epitopes recognized, patient response to vaccine, NV or total (vaccine + NV) peptide epitopes correlated with both PFS and OS, with the exception of NV peptides and PFS, where only a trend was observed (figure 3A). The aggregate frequency of CD8⁺ T cell responses (in IFN- γ ELISPOT assays) appeared better correlated with OS versus PFS for vaccine ($p=0.0052$ vs $p=0.229$), NV ($p=0.0047$ vs. $p=0.109$) and total ($p=0.0016$ vs. $p=0.167$) peptides (figure 3B).

As baseline or on-treatment TCR repertoire diversity has been reported to represent a prognostic indicator of clinical outcome and response to checkpoint blockade in patients with cancer,¹⁷ we next performed TCRseq analyses of patient peripheral blood specimens using the Thermo Fisher Oncomine TCRB-LR Assay.¹⁸ In particular, we focused on determining the relationship of baseline versus on-treatment TCR clonotypic evenness (ie, degree of oligoclonality) and convergence (ie, frequency of non-identical variable-diversity-joining (VDJ) recombination events resulting in identical TCR protein sequence/

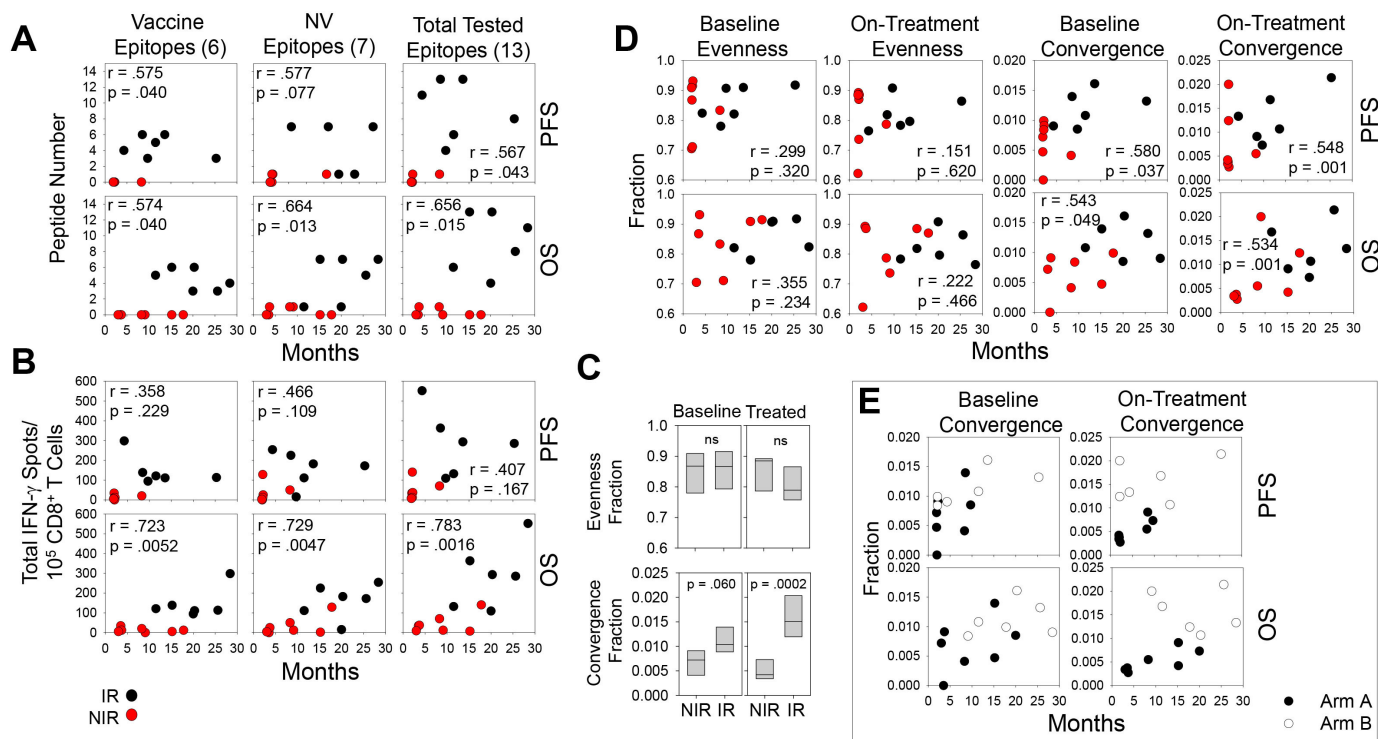


Figure 3 Patient peripheral blood T cell response to vaccine peptides, epitope spreading in the T cell response and baseline TCR convergence are correlated with OCR in treated patients. In (A), patient T cell response to peptide number (vaccine, non-vaccine (NV), total) is plotted as a function of PFS, OS. In (B), aggregate number of spots per 10^5 peripheral blood T cells reactive against screened (vaccine, NV, total) peptides is plotted as a function of PFS, OS. In (C), TCR evenness and convergence in baseline versus on-treatment peripheral blood T cells is reported in immunologic responders (IR) versus patients with no immune response (NIR) to vaccination (as in figure 2A). In (D and E), baseline and on-treatment TCR evenness and convergence are plotted versus patient PFS, OS. In panels (A, B and D), black and red symbols indicate individual patients that were immunologically responsive or non-responsive to vaccine peptides, respectively. In (E), empty versus filled symbols indicate individual patients discriminated by treatment arm. IFN, interferon; OCR, objective clinical response; OS, overall survival; PFS, progression-free survival; TCR, T cell receptor.

antigenic specificity and indicative of antigenic focus) in patients' peripheral T cell repertoires with response to vaccination, OS and PFS. We observed that while evenness in patients' TCR repertoires at baseline or on-treatment failed to correlate with immunologic response to vaccination or to patient PFS or OS (figure 3C,D), TCR convergence was significantly associated with all three of these trial endpoints (figure 3C–E). This was most evident for baseline and on-treatment TCR convergence in the peripheral blood repertoire (figure 3C,D), which was associated with patient immunologic response to vaccination (baseline: $p=0.060$; on-treatment: $p=0.0002$), PFS (baseline: $p=0.037$; on-treatment: $p=0.001$) and OS (baseline: $p=0.049$; on-treatment: $p=0.001$). The highest levels of baseline and on-treatment TCR convergence were observed in patients treated on trial Arm B (baseline: $p=0.047$; on-treatment: $p=0.00015$ for Arm B vs Arm A), in association with superior RECIST V.1.1 OCR (0.0123 ± 0.0026 vs 0.0054 ± 0.0027 , $p=0.0077$ for PR vs PD) and spreading in the T cell repertoire ($p=0.0022$; online supplemental figure S3). Peripheral blood TCR convergence in these treatment-responsive (PR) patients either remained stable or it increased over time (>5 weeks) on treatment (online supplemental figure S4).

These data suggest that α DC1-TBVA peptide-based vaccines were most effective in patients who were immunologically competent to (1) respond to vaccine inclusive peptide epitopes and (2) coordinately develop spreading in their antitumor T cell repertoires. Therapeutic T cell responses were not characterized by the expansion of dominant T cell clonotypes within the peripheral repertoire, but rather with the development of polyclonal populations of T cells exhibiting common specificity (ie, convergence).

α DC1 biomarkers predict patient immunologic response to vaccination and OS

To determine characteristics of the autologous α DC1 cell product that might be associated with patient on-treatment T cell responses against vaccine epitopes (ie, immune response (IR)) and beneficial clinical outcome (ie, PR), patient vaccine DC were phenotypically-profiled and transcriptionally-profiled in exploratory analyses. Levels of cytokines secreted from patient α DC1 were also analyzed by ELISA. We observed that DC expression (%-positive and mean fluorescence intensity (MFI)) of biomarkers traditionally used in α DC1 cell product release criteria, including CD11c, CD14, CD25, CD40,

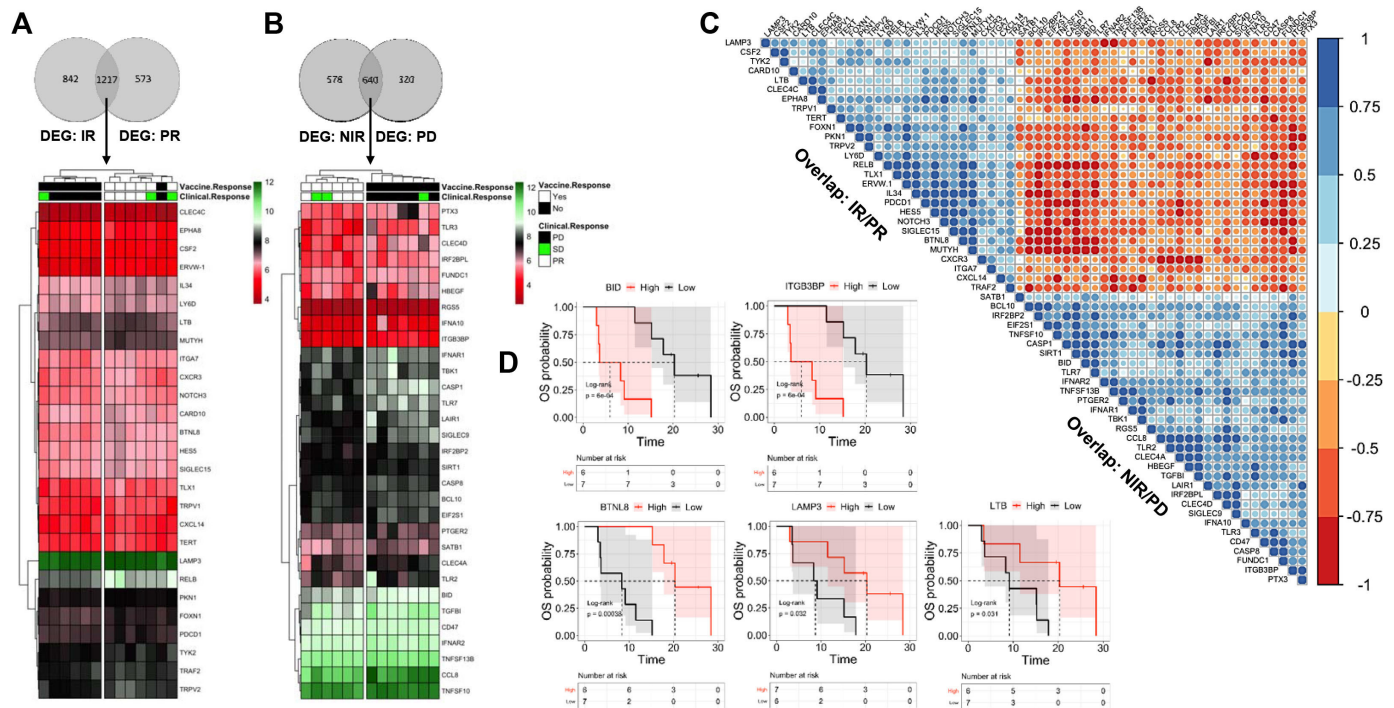


Figure 4 Analysis of α DC1 cells for biomarkers associated with immunologic and clinical response to therapeutic vaccination. Affymetrix gene chips were used to analyze patient α DC1 vaccine cells ($n=13$) for DEG associated with immune response (IR) and PR status to vaccination (A) or no immune response (NIR) and PD status post-vaccination (B), with data reported in depicted heat maps. In (C), a correlation matrix is provided for DEGs associated with preferred treatment outcomes (IR and PR) versus poor outcomes (NIR and PD). In (D), representative DEGs correlated negatively or positively with patient OS are depicted in Kaplan-Meier plots. BID, two times per day; DEG, differentially expressed genes; OS, overall survival; PD, progressive disease; PR, partial response; SD, stabilization of disease; α DC1, autologous type-1 dendritic cells.

CD80, CD83, CD86, CD206, CCR7 and HLA-DR failed to discriminate vaccine DC generated from responders versus non-responders (data not shown). Extended flow cytometry analyses of cell surface costimulatory and checkpoint molecules on vaccine α DC1 similarly failed to identify potential biomarkers associated with treatment outcome, with the possible exception of OX40L, which appeared to be expressed at higher levels on α DC1 from patients who failed to respond immunologically to vaccination (online supplemental figure S5; $p = 0.035$). Analyses of levels of interleukin (IL)-12p70 and IL-10 secreted by vaccine α DC1 did not identify differences associated with patient immunologic or clinical response to treatment (data not shown).

Using Affymetrix gene chip profiling, we then compared α DC1 between patients differing in immunologic response to vaccine peptides (based on IFN- γ ELISPOT assays) and OCR (figure 4). We identified 2059 and 1790 DEG positively associated with T cell responses and PR status on-trial, respectively, with 1217 overlapping DEG identified in these cohorts (figure 4A). Examples of overlapping DEG with high correlations with extended OS included *BTNL8*, *CSF2/GMCSF*, *CXCL14*, *CXCR3*, *IL34*, *IRF3*, *LAMP3*, *LTB*, *LY6D*, *PKN1*, *RELB*, *TRAF1* and *TRAF2*, among others (figure 4A,C and D). Conversely, α DC1 transcripts associated with patient lack of immunologic response, disease progression and shorter OS

included *BID*, *CD47*, *CLEC4C*, *IL18BP* (encoding an IL-18 decoy receptor), *ITGB3BP*, *LAIR*, *PTGER2*, *SIRT1*, *SATB1*, *TGFBI*, and interestingly, *RGS5* (one of the TBVA targeted in this vaccine trial), among others (figure 4B–D). Gene set enrichment analyses (GSEA) supported the predominance of gene signatures associated with deficiency in antigen-presenting cell function, IFN/Toll-like receptor (TLR)/IL1 family cytokine signaling and pyruvate metabolism/tricarboxylic acid (TCA) cycle in vaccine α DC1 from NIR/PD versus IR/PR patients (online supplemental figure S6).

Vaccine efficacy is only moderately inversely correlated with changes in regulatory immune cell populations

As we had previously observed that combination vaccines + dasatinib reduced MDSC and Treg frequencies in murine melanoma models,¹² with others reporting that dasatinib reduced circulating levels of MDSC and Treg in treated patients with chronic myeloid leukemia,^{19 20} we monitored these immune cell populations in patient peripheral blood on-treatment by flow cytometry. As shown in online supplemental figure S7, peripheral blood CD4⁺Foxp3⁺ Treg frequencies failed to differ at baseline versus on-treatment (at week 5) between immunologic responders and non-responders to vaccination or between treatment Arms A and B (data not shown). There was a trend ($p=0.092$) for reduced levels of Treg in PR versus PD patients, and a statistical difference observed for

reduced Treg in PR versus SD ($p=0.029$) patients on-treatment (online supplemental figure S7B). Except for higher levels of HLA-DR^{neg}CD11b⁺CD14⁺CD15^{neg}CD33⁺ monocytic MDSC (M-MDSC) in PR versus PD ($p=0.021$) and PR versus SD (trend $p=0.091$) patients at baseline, no other significant differences in M-MDSC and HLA-DR^{neg}CD11b⁺CD14^{neg}CD15⁺CD33⁺ PMN-MDSC subsets were observed in patient blood that correlated with immunologic response to vaccination, treatment arm or OCR status (online supplemental figure S7 and data not shown).

Serum analyses for biomarkers of vaccine efficacy

Based on our translational findings for increased *in vivo* production of the pro-inflammatory chemokine CXCL10 in B16 melanoma-bearing mice treated with combination vaccines + dasatinib,¹² and reports for predictive changes in levels of CXCL10 and soluble checkpoint molecules in the serum/plasma of patients with melanoma effectively treated with immunotherapy,^{21,22} we analyzed levels of these factors in patients at baseline and at week 5 on-treatment. We observed no significant association in serum concentrations of CXCL10 (online supplemental figure S8) or soluble costimulatory/checkpoint molecules (online supplemental figure S9) with immunologic response to vaccination or clinical outcomes.

Activation of intratumoral immunity predicts vaccine clinical activity

Given limiting quantities of tumor biopsy tissue obtained from patients in the current trial, formal histopathologic analyses of vascular normalization, tissue hypoxia, immune cell infiltration and TLS as anatomic structures within the TME could not be performed. Instead, transcriptional profiling was performed on the available biopsy material, including matched baseline and on-treatment tissues from 12 patients (4 PR, 2 SD and 6 PD). Messenger RNA extracted from tumor specimens was analyzed using the OIRRA detecting 395 targets relevant to immune-oncology, and a custom-designed NanoString panel targeting selected gene products associated with TLS formation.

As shown in figure 5A, hierarchical clustering of selected, significant ($p<0.05$, Wilcoxon test) differentially expressed genes (OIRRA) in baseline tumor biopsies was performed, allowing for segregation of patients based on immunologic and clinical response to treatment. A correlation matrix (figure 5B) was then developed to highlight baseline tumor transcripts associated with best patient outcomes (ie, immune response to vaccination and clinical PR; $n=4$) versus worst patient outcomes (ie, lack of immune response and clinical PD; $n=6$). Melanomas in patients responding to the combination vaccine were characterized by genes associated with innate/adaptive immune cell function (*CBLB*, *CD48*, *IL2RG*, *GLNY*, *KIR2DL2*, *NCR1*, *NCR3*, *SRGN*), antigen presentation (*CD80*, *CD86*, *CD226*, *HLA-DMB*, *ICOSLG*, *ITGAM*, *ITGB2*) and inflammation/immune cell recruitment

(*CCL3*, *CCR5*, *CD274/PD-L1*, *CMKLR1*, *IFIH1*, *ITGB7*), while baseline tumors in patients who fared poorly on trial expressed elevated levels of transcripts encoding the anti-apoptotic protein *BCL2* and *CA4*, a biomarker of tissue acidosis/hypoxia²³ (figure 5B,C). Baseline tumor *BCL2* and *CA4* expression appeared most strongly negatively associated with *CBLB* and *KIR2DL2* expression (figure 5B). GSEA further revealed baseline enrichment in gene signatures associated with the adaptive immune system, cellular interactions with the vasculature and immunoregulatory interactions between immune and non-immune cell types among patients with IR/PR versus NIR/PD, and conversely enrichment in a (tumor) cell cycle gene signature in patients with NIR/PD versus IR/PD (online supplemental figure S10).

Similar analyses were then performed to determine on-treatment changes in tumor transcriptional profiles associated with therapy outcomes (figure 5D–F). OIRRA-based analyses (figure 5D,E) revealed that tumors in patients that responded immunologically and clinically to vaccination ($n=4$) became enriched in DEGs associated with inflammatory innate/adaptive immune cell infiltration (*CCL2*, *CD22*, *CX3CL1*, *FCGR3A*, *GNLY*, *HLA-DQB2*, *ID3*, *JAML*, *KIR2DL2*, *MRC1*, *S100A8*, *S100A9*). Conversely, as shown in figure 5D–F, tumors in patients that progressed on trial ($n=6$; all of whom failed to respond immunologically to vaccination) were enriched in DEGs associated with tissue hypoxia (*HIF1A*), glycolysis (*IRS1*), tumor cell proliferation/renewal and DNA repair (*BRCA2*, *KIAA0101*, *MELK*, *MKI67*, *TOP2A*), tumor cell metastasis (*ITGAE*) and immune suppression (*PTPN11*). Correlation matrix analyses suggest strongest general negative associations between *IRS1* and *PTPN11* with on-treatment biomarkers linked to immune/clinical response to vaccination (figure 5E). GSEA supported on-treatment enrichment in gene signatures associated with adaptive and innate immunity, (MHC I) antigen processing and cross-presentation, immune interactions with blood vessels and neutrophil degranulation in patients with IR/PR versus NIR/PD (online supplemental figure S10). As was the case for baseline tumor analyses, a (tumor) cell cycle gene signature was enriched in patients with NIR/PD versus IR/PD (online supplemental figure S10).

Development of a TLS transcriptional profile in tumors on-treatment predicts immunologic/clinical outcomes

Based on recent reports linking patient with melanoma response to immunotherapy with the presence or treatment-induced formation of tertiary lymphoid structures (TLS) within the TME,^{24–26} we developed a custom NanoString probe set for 23 TLS-associated genes and analyzed RNA isolated from patient tumor biopsies at baseline and for changes in transcript expression on-treatment. While baseline profiling of TLS-associated gene transcripts was not predictive of subsequent patient response to vaccination (figure 6A), hierarchical clustering of TLS-associated DEGs segregated patients with

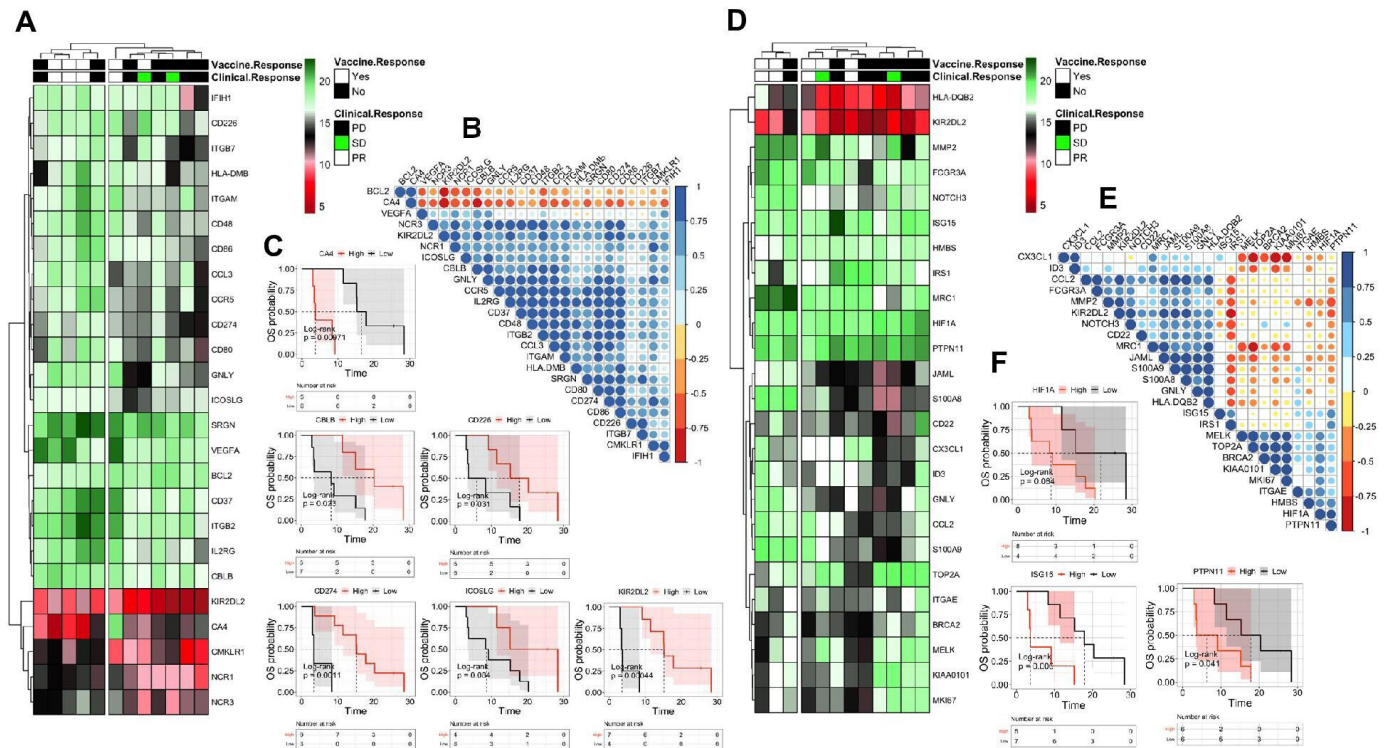


Figure 5 Transcriptional profiling of tumor biopsies for predictive DEG associated with patient outcomes on trial. OncoPrint Immune Response Research Assay profiling of tumor biopsy tissues was performed as outlined in Materials and Methods. Hierarchical clustering of selected, significant ($p < 0.05$, Wilcoxon test) DEGs in patient baseline (A) and on-treatment (D) tumor biopsies ($n=12$) is shown. The genes shown were selected from two individual differential expression analyses: (1) PR versus PD and (2) (vaccine-induced, antigen-specific) immune response (IR) versus no immune response (NIR). Data is clustered by objective clinical response and immune response of each patient. Rows represent individual genes and columns represent individual patient tumor samples. Gene expression is expressed as log₂ normalized read counts. Correlation matrices for baseline (B) and on-treatment (E) tumor DEG associated with IR/PR versus NIR/PD are depicted. Spearman's correlation coefficients were calculated. Positive and negative correlations are shown in blue and red, respectively. The size of the circle and color intensity are proportional to the calculated Spearman's correlation coefficient. Kaplan-Meier estimates of survival based on the expression of representative baseline (C) and on-treatment (F) tumor DEGs are reported. The logrank test was used to test the significance and censored patients were indicated by a vertical line. The median survival for each group is indicated by the dotted line. DEG, differentially expressed genes; OS, overall survival; PD, progressive disease; PR, partial response; SD, stabilization of disease.

vaccine/clinical responses versus those with progressive disease that failed to respond immunologically to the vaccine (figure 6B). Specifically, as shown in figure 6B,C, only patients with positive outcomes displayed increased on-treatment expression of gene transcripts linked to TLS formation (*CCL19*, *CCL21*, *LTA*, *LTB*, *TNFSF14*), high endothelial venule development (*CHST2*, *FUT4*), immune cell infiltration and inflammation (*CD8A*, *CD20*, *CD274*, *CXCL10*, *IFNG*, *LAMP3*, *TBX21*). Patient #13 (SD, immunologic non-responder) clustered with PD patients in exhibiting a deficiency in expression of TLS-associated biomarker transcripts. Furthermore, we noted that the emergence of a TLS biosignature in the therapeutic TME was strongly correlated ($p < 0.001$) with epitope spreading in the peripheral CD8⁺ T cell repertoire (figure 6D,E). Hence, while we were unable to assess histopathologic presence of TLS in situ due to limited amounts of tumor biopsy tissue, these data suggest that effective vaccination against TBVA may promote a therapeutic TME

characterized by a TLS transcriptional bio-signature and epitope spreading in the peripheral T cell repertoire.

DISCUSSION

In this pilot phase II trial, we observed that treatment of advanced, patients with checkpoint-refractory melanoma with an autologous α DC1-based vaccine targeting TBVA together with a TME conditioning agent (dasatinib) was safe, immunogenic and therapeutically effective. These results parallel findings in our preclinical tumor models.¹² AEs were consistent with those observed in previous clinical studies of dasatinib monotherapy,^{27,28} with no discernable impact from the vaccine component in the combination regimen, as one would predict from the consensus safety profile (ie, grade 1–2 skin reactions, flu-like symptoms) for past DC/peptide-based vaccines administered alone or in combination with alternate interventional agents.²⁹

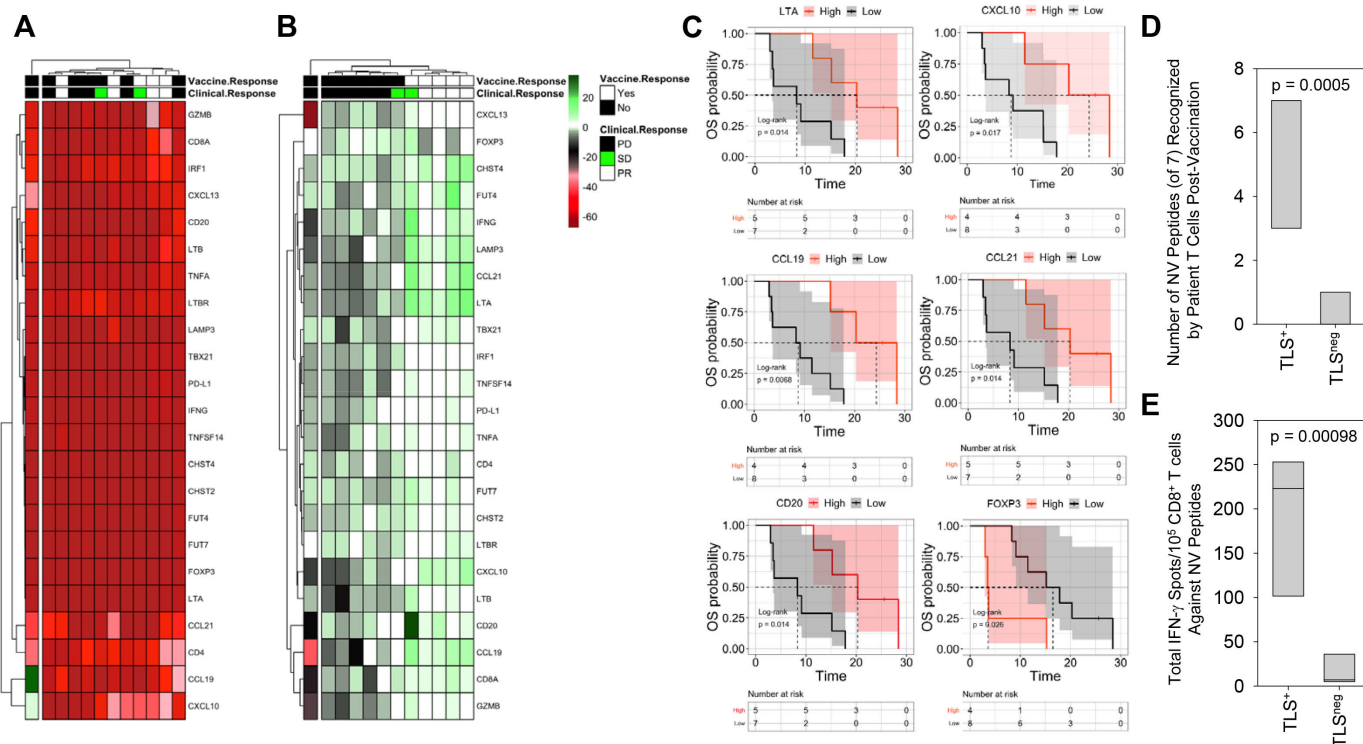


Figure 6 Acquisition of TLS-associated DEG in the tumor microenvironment on-treatment predicts patient immunologic/clinical response to therapeutic vaccination. Tumor biopsies isolated at baseline and 5 weeks after beginning treatment were processed to recover total RNA which was analyzed using a custom NanoString array targeting pro-inflammatory/pro-TLS transcripts, as outlined in Materials and methods. Hierarchical clustering of selected, significant ($p < 0.05$, Wilcoxon test) DEG in patient baseline tumor tissues (A) or from on treatment versus baseline time points (B) are depicted ($n = 12$ in both cases). The data are clustered based on the OCR and IR status of each patient. Rows represent individual proteins and columns represent individual patients. In (C), Kaplan-Meier estimates of survival based on the expression of representative DEGs associated with changes in immunologic/clinical response on-treatment are reported for LTA, CXCL10, CCL19, CCL21, CD20 and Foxp3. Patient peripheral blood T cell response to non-vaccine (NV) peptides (as reported in figure 2A, online supplemental figure S3A,B) based on total number of NV peptides reacted against (D) and total IFN- γ spots/ 10^5 CD8 $^+$ T cells against NV peptides (E) and were plotted versus patient on-treatment TLS status based on biomarker signature. Patients with TLS biosignatures (TLS $^+$; $n = 5$; Pt. #'s 1, 2, 5, 9, 14). Patients without TLS biosignatures (TLS $^{\text{neg}}$; $n = 7$; including Pt. #'s 4, 6, 7, 10, 12, 13, 15). Differences between groups were determined by student t-test. IFN, interferon; IR, immune response; OCR, objective clinical response; OS, overall survival; PD, progressive disease; PR, partial response; Pt., patient; SD, stabilization of disease; TLS, tertiary lymphoid structure.

Given previous reports for clinical efficacy of DC-based vaccines being associated with patient with melanoma T cell responses against multiple versus single target epitopes,³⁰ our primary endpoint required patient T cell reactivity against three or more vaccine peptides for designation as a positive response. Six of 13 evaluable patients developed specific CD8 $^+$ T cell responses to ≥ 3 vaccine peptides on-treatment (ie, 46% IRR), with all of the immunologic responder patients exhibiting preferred clinical outcomes (ie, 4 PR and 2 SD). Notably, in patients responding to vaccination, anti-TBVA peripheral blood T cell responses undulated over time on treatment, consistent with results from prior DC-based vaccine trials^{31–33} and suggestive of reiterative temporal rounds of specific T cell cross-priming and recruitment of vaccine-induced T cells from blood into the TME. Conversely, seven evaluable patients who failed to respond to vaccination had comparatively poor clinical outcomes (one SD and six PD). Remarkably, patients treated on Arm B developed superior outcomes versus

patients treated on Arm A with respect to IRR (66.7% vs 28.6%), ORR (66.7% vs 0%), OS (median 15.45 vs 3.47 months) and PFS (median 7.87 vs 1.97 months). By comparison, a phase II study of dasatinib (70mg two times per day) monotherapy in 51 evaluable patients with advanced-stage melanoma yielded an ORR of 5.9%, with median OS and PFS of 7.5 and 2.1 months, respectively.²⁷

The observed inter-cohort differences in immunologic/clinical outcomes could reflect the benefit of dasatinib administered during the initial vaccine priming phase of therapy for patients on Arm B versus Arm A, with the latter patients receiving vaccine alone for the first cycle of treatment. In this regard, dasatinib has been previously reported to enhance specific T cell cross-priming and to improve OS in murine tumor (melanoma, breast carcinoma) models treated with combination vaccine protocols.^{12, 34} Dasatinib is also known to improve innate pro-inflammatory natural killer (NK) effector cell activity³⁵ and to enhance the immunostimulatory capacity of DC,³⁶ while coordinately reducing

levels of immunoregulatory cell populations such as Treg and MDSC in the TME of treated animals.¹² Any of these drug-associated effects would be anticipated to augment DC-mediated CD8⁺ T cell cross-priming *in vivo*.³⁷ With these caveats, we observed that while the magnitude of peak T cell responses against vaccine and non-vaccine peptides did not differ significantly between the immunologic responders in Arm A versus Arm B (data not shown), the kinetics of patient T cell responses were strikingly different based on treatment arm. On-treatment time to first detection of positive patient T cell response against vaccine peptides was 3.5±1.0 weeks in Arm B versus 8.5±0.7 in Arm A ($p=0.0035$, *t*-test), while time to first detection of positive patient T cell response to non-vaccine peptides was 3.9±1.1 weeks in Arm B versus 9.5±0.7 weeks in Arm A ($p=0.0018$, *t*-test). This temporal shift in patient response between the two treatment arms roughly approximates to the delay in initiating dasatinib administration as a co-therapeutic agent/vaccine adjuvant to patients treated on Arm A, suggesting the importance of dasatinib in enabling vaccine-induced T cell (cross)priming by the combination regimen.

Counterintuitively, dasatinib can also (reversibly) inhibit lymphocyte cell-specific protein-tyrosine kinase (LCK), a Src-family tyrosine kinase required for effective TCR-mediated signaling in T cells.³⁸ In this regard, it has been suggested that transient interruption of TCR signaling in the cancer setting may be beneficial to sustaining antitumor T cell fitness and preventing T cell apoptosis due to chronic antigen-specific stimulation.¹² Expanded studies evaluating the fitness and polyfunctionality of therapeutic T cells in the periphery and the TME of treated individuals will be required to address these mechanistic possibilities in future dasatinib-based combination immunotherapies.

An alternate or additional consideration impacting the apparent superior efficacy of the Arm B regimen in our study may reflect an imbalance in male/female composition among evaluable patients in the two treatment arms (ie, 2/7 (28%) women in Arm A vs 3/6 (50%) women in Arm B). As such, the data could support possible gender bias in IRR (80% vs 25%) and ORR (60% vs 12.5%) favoring female versus male patients treated on the Arm B versus Arm A regimens, respectively. Interestingly, a growing literature argues for the convention that women (and males with hypogonadism) exhibit stronger pro-inflammatory responses when compared with intact men, with women at higher risk to develop autoimmune-related pathologies.^{39–41} Indeed, 80% of systemic autoimmune diseases have been reported to occur in women.⁴¹ Relevant to the UPCI 12-048 trial, women have also been reported to respond more robustly than men to vaccination in the infectious disease setting,^{39–40} in murine tumor models receiving anti-PD-1 checkpoint blockade immunotherapy,⁴² and in patients with melanoma with low-moderate levels of partially-exhausted cytotoxic CD8⁺ T lymphocytes receiving combination anti-PD-1-based immunotherapies.^{43,44} Such female versus male dominance in response to immunotherapy has been correlated to sex-associated differences in the microbiome,^{45,46} gene-dosing

effects of X-chromosome-linked immune gene products, and the comparative immunostimulatory versus immunoregulatory action of estrogens versus androgens, respectively.⁴³ However, there are reports that clearly support an opposing viewpoint for the superior efficacy of vaccines and checkpoint blockade-based interventions in men versus women.^{47–48} These contrasting results may relate to the specific immune pathways primarily targeted by the applied regimens, with gender-dimorphism in the targeted pathways dictating differential outcomes to treatment between the sexes. Given the greater incidence of solid cancers in men versus women,⁴⁹ it will be important that prospective translational and clinical studies of (combination vaccine) immunotherapies be designed in accordance with sex and gender equity in research guidelines.⁵⁰ Furthermore, confounding variables such as age, sex hormone concentrations, hormone replacement therapies, body mass index and menopausal status should be factored into the analysis and interpretation of future study outcomes as potential covariates.

Our trial included patients with cutaneous, mucosal and uveal melanoma, with the latter indications notoriously difficult to treat with interventional therapies, including immunotherapies.⁵¹ Notably, the demographics of patient site of primary melanoma differed between the treatment arms (figure 2A, online supplemental table S1) which could conceivably impact vaccine outcomes, with Arm A containing a higher frequency of patients with uveal melanoma (44.4% vs 16.7% in Arm B) and mucosal melanoma (11.1% vs 0% for Arm B) and Arm B containing more patients with cutaneous melanoma (83.3% vs 44% in Arm A). However, IRR was greater for both cutaneous (60% vs 0%) and uveal (100% vs 25%) patients with melanoma treated on Arm B versus Arm A, and PR to treatment was observed in 60% versus 0% of patients with cutaneous melanoma and 100% versus 0% of patients with uveal melanoma treated on Arm B versus Arm A (figure 2A). These data suggest that the Arm B treatment regimen may be superior to Arm A irrespective of the patient's site of primary disease.

As was the case in foundational murine melanoma modeling developed using this combined vaccine approach,¹² we observed that patients that coordinately developed CD8⁺ T cell responses against multiple vaccine peptides and OCR also displayed evidence for expanded T cell reactivity against antigens that were not targeted in the vaccine, but which are considered disease-relevant as they derive from known melanoma differentiation antigens or TBVA. Such DC-dependent spreading in the peripheral T cell repertoire has been previously reported to occur in patients exhibiting OCR after treatment with a range of immunotherapies (ie, vaccines, gene therapies, checkpoint blockade, recombinant cytokines; online supplemental table S1).^{14,15,52} In such cases, the extended T cell response against tumor (differentiation, oncofetal, mutated neo-) antigens is believed to improve immune-mediated control of antigenically-diverse tumor lesions, providing an operational improvement in immune

surveillance over that enforced by vaccine-specific T cells or adoptively-transferred monospecific T cells.^{14 52 53}

As an alternate means to assess changes in the patient's T cell repertoire on trial, coordinate profiling of TCRV β chain transcripts was performed. In contrast to several recent reports associating baseline/on-treatment peripheral blood TCR clonotypic evenness with improved PFS, OS, ORR and/or OCR in trials administering cancer vaccines or checkpoint blockade,^{17 54} we did not observe a significant association between baseline or on-treatment TCR evenness in peripheral blood with patient responsiveness to vaccination, PFS, OS or OCR (figure 3). However, we did identify significant associations between TCR convergence (indicative of antigen-driven responses) and IRR, PFS, OS and OCR in baseline and (particularly) on-treatment peripheral blood specimens that were analyzed (figure 3). These findings are similar to those reported by Naidus *et al*⁵⁵ where peripheral blood TCR convergence was directly correlated to patient OS after PD-L1 blockade in patients with advanced-stage non-small cell lung cancer. These data suggest that TCR convergence in peripheral blood T cells may represent an actionable biomarker for (1) identification of patients most likely to respond to immunotherapeutic interventions that mechanistically require T cell responses to achieve preferred clinical outcomes and (2) effective longitudinal monitoring of therapeutically meaningful T cell responses in patients on-treatment.

One major unresolved question for the field of DC-based vaccines relates to the identification of biomarkers associated the ability of injected DC to elicit therapeutic anti-tumor T cell responses in treated patients. Although all patient-derived type-1-polarized α DC1 were generated using a standard operating protocol and passed release criteria for use in vaccine formulations, consistent with recent reports,^{15 56} we observed that none of the markers used to traditionally qualify vaccine DC (ie, CD11c, CD14, CD25, CD40, CD80, CD83, CD86, CD206, CCR7, HLA-DR, IL-12p70 production, IL-10 production, IL-12p70/IL-10 ratio) were correlated with patient specific T cell or clinical responses. Extended analysis of costimulatory/co-inhibitory molecules on vaccine α DC1 cells by flow cytometry similarly failed to demonstrate associations with patient response to vaccination (online supplemental figure S5), with the exception of OX40L which appeared to be expressed at higher levels on α DC1 generated from patients that failed to respond to vaccination. In this context, it is interesting to note that subsets of OX40L⁺ DC have recently been reported to selectively promote Treg expansion⁵⁷ and melanoma progression.⁵⁸

Despite our general inability to identify potential vaccine bioefficacy markers using protein-based methods, Affymetrix gene chip transcriptional profiling of patient-generated vaccine DC revealed possible associations between preferred outcomes (ie, IRR and OCR) with biomarkers linked to DC maturation (ie, *CSF2/GMCSF*, *LAMP3*, *RELB*), naïve T cell priming by antigen presenting cells (ie, *BTNL8*), pro-inflammatory

immunity/Type-1 IFN signaling (ie, *CXCL14*, *CXCR3*, *IL34*, *IRF3*, *PKN1*), cell survival (ie, *TRAF1*, *TRAF2*) and intriguingly, the formation of lymphoid structures (ie, *LTB*, *TLXI*).^{59 60} Conversely, vaccine DC associated with superior patient IRR/OCR were deficient in expression of gene products associated with immune cell apoptosis (ie, *BID*), immature DC (ie, *CD47*, *ITGB3BP*) or immune suppression/tolerance (ie, *IL18BP*, *LAIR*, *PTGER2*, *RGS5*, *SATB1*, *TGFB1*).^{61 62} Gene signature analyses suggested inferiority in overall α DC1 functionality in patients with NIR/PD (online supplemental figure S6). Validation of these DC vaccine biomarkers for their capacity to predict patient IRR/OCR on-treatment will need to be carefully evaluated within the context of immunologic monitoring in future clinical trial designs.

Transcriptional profiling of tumor biopsies at baseline revealed several potential biomarkers associated with immunologic and clinical response to autologous α DC1-based vaccination in the current trial, with GSEA suggesting existing adaptive immune presence as predictive of patient IR/PR status on-treatment (online supplemental figure S10). Consistent with several recent reports, expression of CD274/PD-L1 in baseline tumors appeared predictive of patient response to our immunotherapeutic intervention.⁶³ These immunologically 'hot' tumors also expressed high levels of a range of transcripts associated with recruitment of inflammatory innate immune effector cells (*CCL3*), including NK and innate lymphoid cells (*KIR2DL2*, *NCR1/NKp46*, *NCR3/NKp30*), secretory/cytolytic cells (*GLNY*, *SRGN*) and antigen presenting cells (*CD80*, *CD86*, *CD226*, *HLA-DMB*, *ICOSLG*, *ITGAM*, *ITGB2*) into a TME that is deficient in acidosis/hypoxia based on reduced expression of *CA4*.²³ That CBLB expression in baseline tumors was associated with superior response to treatment was somewhat surprising as this E3-ligase has been previously reported to negatively regulate the function of immune cells, including CD8⁺ T cells and DC.⁶⁴ One possible explanation for our observations may reflect the reported need for Src family kinase activation of CBLB for its reported immunoregulatory activity.⁶⁵ Hence, provision of the Src inhibitor dasatinib within the context of our combined immunotherapy might be envisioned to release immune cells from CBLB-mediated suppression in support of beneficial immune-mediated treatment outcomes.

Molecular changes in the TME associated with response to vaccination (IR, OCR) included a reduction in hypoxia (*HIF1A*) and glycolysis (*IRS1*) indices, consistent with the expectation for vascular normalization as an endpoint for this vaccine approach targeting TBVA.⁸⁻¹⁰ A strengthening of transcript profiles associated with immune cell recruitment (*CCL2*, *CX3CL1*, *JAML*), and a more diversified immune cell profile including B cells (*CD22*), DC/macrophages/monocytes (*MRC1*, *S100A8*, *S100A9*), NK cells (*FCGR3A/CD16*, *KIR2DL2*) and secretory/cytotoxic cells (*GNLY*) was observed in the tumors of patients responsive to treatment. Based on reduced levels of *PTPN11/SHP2* transcript expression in the tumors of responding

patients, one may also hypothesize that immune cells within the therapeutic TME may be less encumbered by regulatory signaling molecules containing ITIM motifs, including checkpoint and KIR molecules.^{66, 67} Surprisingly, OIRRA-based profiling suggested that lower levels of *ISG15* transcript expression in the TME on-treatment were linked to superior OS (figure 5F). Although *ISG15* protein has been reported to serve as an effective adjuvant to vaccination,⁶⁸ it is also known to represent a biomarker of poor prognosis in the cancer setting⁶⁹ and to mediate pro-tumor immunoregulatory activity.⁷⁰ GSEA supported enhanced vascular-immune crosstalk, innate and adaptive immune cell presence, and antigen-presenting cell function in the TME of patients with IR/PR versus NIR/PD on trial (online supplemental figure S11).

Complementary NanoString-based transcriptional profiling clearly distinguished patients that performed well on trial (IR, OCR) versus patients that failed to respond to the vaccine either immunologically or clinically (figure 6B). Responding tumors transcript profiles were enriched in biomarkers of inflammation (*CD274*, *CXCL10*, *IFNG*, *IRF1*, *TBX21*, *TNFA*), cytotoxic effector cells (*GZMB*) and tertiary lymphoid structures (*CCL19*, *CCL21*, *CD8A*, *CD20*, *CHST4*, *CXCL13*, *FUT4*, *LAMP3*, *LTA*, *LTB*, *TNFSF14*). These findings are consistent with recent reports supporting the association of TLS neogenesis in the TME with favorable clinical response to immunotherapy.^{24, 25} It is also interesting to speculate that therapeutic TLS formation in the TME may serve as a center for expanded T cell cross-priming and spreading in the antitumor CD8⁺ T cell repertoire, since these events were strongly correlated in this trial ($p=0.0005$ and $p=0.00098$, respectively; figure 6D,E).

Finally, it is worth noting that all patients treated on this trial had previously received at least one form of prior immunotherapy, including rIL-2, rIFN α , checkpoint blockade and/or vaccines (online supplemental table S1). We observed no apparent impact of prior treatment on patient outcomes on the current trial, with five of the six immunologic/clinical responders having demonstrated primary and/or acquired resistance to prior treatment with checkpoint blockade, and the remaining responder (ie, patient #14) being checkpoint treatment naive (figure 2A). Four patients, including three on treatment Arm A (ie, patients #4, #7, #9) and patient #5 treated on Arm B had received previous autologous DC-based vaccines (ie, adenovirus-engineered DC expressing MAGE-6, MART1 and tyrosinase; online supplemental table S1), however, the vaccine antigens used in the previous trial and the current trial do not overlap and we observed no baseline T cell responses against TBVA antigens in these patients (assuming spreading might could have occurred in T cell responses as a consequence of the prior vaccination regimen).

The authors acknowledge several limitations in this phase II clinical trial including its small sample size, its inclusion of advanced stage patients with cutaneous, mucosal or uveal forms of melanoma, and the characterization of the

therapeutic TME which was restricted to use of transcriptional profiling rather than tissue imaging technologies (particularly in the context of TLS). Our findings must be confirmed in larger cohort studies in future trials. In this regard, we plan to extend our investigation of α DC1/TBVA peptide-based vaccines in two NIH-supported, prospective phase II clinical trials to be initiated in 2021. In one trial (NCT04093323), up to 24 advanced-stage HLA-A2⁺ patients with melanoma with primary resistance to anti-PD-1 will be treated with autologous α DC1/TBVA and a systemic chemokine modulating regimen (ie, combined IFN α_2 , rintatolimod, celecoxib) designed to enhance vaccine-induced TIL recruitment and to potentially support enhanced TLS formation by sustaining inflammation in the therapeutic TME. In the other trial, up to 21 patients with early-stage HLA-A2⁺ with clear-cell renal cell carcinoma will receive autologous α DC1/TBVA peptide-based vaccination combined with low-dose cabozantinib in the neoadjuvant setting beginning 6 weeks prior to planned surgery, with tumors evaluated for treatment-associated changes in size, vascular structure, immune infiltration, TIL TCR repertoire and TLS formation.

In summary, our data support the safety and immunogenicity of vaccination against non-mutated TBVAs overexpressed by the tumor-associated vasculature, and they provide a preliminary indication of the therapeutic efficacy of this treatment approach in patients with checkpoint-refractory disease particularly when combined with early dasatinib co-administration. Since the TBVAs targeted in this trial are overexpressed in multiple cancer types, these outcomes have implications for future vaccine protocols designed to treat patients with diverse forms of solid, vascularized tumors.

Author affiliations

¹Dermatology and Immunology, University of Pittsburgh School of Medicine, Pittsburgh, Pennsylvania, USA

²Translational and Regulatory Affairs, Parker Institute for Cancer Immunotherapy, San Francisco, CA, USA

³Biostatistics, University of Pittsburgh Graduate School of Public Health, Pittsburgh, Pennsylvania, USA

⁴Biostatistics, UPMC Hillman Cancer Center, Pittsburgh, Pennsylvania, USA

⁵Immunoregulation and Immunodiagnosics, Chittaranjan National Cancer Institute, Kolkata, West Bengal, India

⁶Immunotherapeutics and Biotechnology, Texas Tech University Health Sciences Center, Abilene, Texas, USA

⁷Clinical Research Services, UPMC Hillman Cancer Center, Pittsburgh, Pennsylvania, USA

⁸Medicine, University of Pittsburgh School of Medicine, Pittsburgh, Pennsylvania, USA

⁹Medicine, UPMC Hillman Cancer Center, Pittsburgh, Pennsylvania, USA

¹⁰Immunology, University of Pittsburgh School of Medicine, Pittsburgh, Pennsylvania, USA

¹¹Microbiology and Immunology, LECOM, Greensburg, Pennsylvania, USA

¹²Immunology, Singular Genomics, Austin, Texas, USA

¹³Molecular Biology, Thermo Fisher Scientific, Santa Clara, Carlsbad, California, USA

¹⁴Medical Oncology and Immunology, Roswell Park Cancer Institute, Buffalo, New York, USA

¹⁵Research and Development, Parker Institute for Cancer Immunotherapy, San Francisco, California, USA

¹⁶Microbiology and Immunology, University of California San Francisco, San Francisco, California, USA

¹⁷Cutaneous Oncology and Immunology, Moffitt Cancer Center, Tampa, Florida, USA

¹⁸Melanoma Medical Oncology, University of Texas MD Anderson Cancer Center, Houston, Texas, USA

¹⁹Medicine, University of Pittsburgh, Pittsburgh, Pennsylvania, USA

Twitter Hussein Tawbi @HTawbi_MD

Acknowledgements The authors wish to thank members of our Clinical Research Services (Barbara Stadterman, MPH, CPH, MSCR, CCRP and Mary Horak, BS, CCRP) and our Education and Compliance Office (Nita Missig Carroll, RN, BSN, OCN, CCRC) and Mr Josh Plassmyer for their assistance in protocol performance, regulatory compliance and clinical data analysis, respectively. We also wish to acknowledge the UPMC Hillman Immunologic Monitoring and Cellular Products Laboratory (sustained in part by P30 CA047904) for their outstanding support in DC vaccine manufacture and exploratory serum analyses, and the University of Pittsburgh Genomics Core Facility for their assistance in transcriptional profiling studies. We thank Drs Joseph Baar and Louis D Falo for their critical comments and suggestions made during the preparation of this manuscript.

Contributors Patient enrollment and management: AT, HT, JMK. Protocol coordination and assignment to treatment arm: AR, MD. Designing research studies: WJS, AB, DL, PK, LHB, HT. Conducting laboratory experiments: DM, JLT, MC, RJF, LM, EL. Acquiring data: DM, AR, MD, LK, JLT, MC, RJF, GML, LHB, AT, HT, JMK. Analyzing data: WJS, DM, YL, FD, JLT, MC, RJF, JNF, TJL, AT, HT, JMK. Writing/editing the manuscript: All authors. Guarantor: WJS.

Funding These studies were supported by NIH R01 CA169118 (to WJS), NIH R01 CA204419 (to WJS) and NIH P01 CA234212 (to WJS and PK).

Competing interests WJS, DM, YL, FD, LK, AB, DBL, AR, MD, JLT, MC, RJF, JNF and PK declare no competing interests. TJL was an employee of Thermo Fisher Scientific during the performance of this work. TJL, LM, EL and GML are/were employees of Thermo Fisher Scientific during the performance of this work. LHB declares the following unrelated advisory activities: StemImmune/Calidi Scientific and Medical Advisory Board, April 6, 2017–present; SapVax Advisory Board meetings November 15, 2017; December 6, 2018; NextCure, Scientific Advisory Board, 2018–2020; Western Oncolytics, Scientific Advisory Board, 2018–present; Torque Therapeutics, Scientific Advisory Board, 2018–2020; Khloris, Scientific Advisory Board, 2019–present; Pyxis, Scientific Advisory Board, 2019–present; Cytomix, Scientific Advisory Board, 2019–present; Vir, Scientific Advisory Board meeting, February 2020; DCprime, Scientific Advisory Board meeting, November 2020; RAPT, Scientific Advisory Board, 2020–present; Takeda, Scientific Advisor, 2020–present; EnaraBio scientific advisor, February 2021. AT declares the following unrelated advisory activities: Receipt of fees for consulting and/or advisory board participation from Partner Therapeutics, Merck, Bristol Myers Squibb, Novartis, Genentech-Roche, Array Biopharma, Sanofi-Genzyme/Regeneron, Pfizer, EMD Serono, NewLink Genetics, BioNTech, Immunocore, and Eisai; participation in a Data Safety Monitoring Board for Incyte; involvement with institution contracted research with Merck, OncoSec, Genentech-Roche, Bristol Myers Squibb, Amgen and Clinigen. HT declares the following unrelated consulting Honoraria: BMS, Novartis, Merck, Genentech, Eisai, lovance, Boxer Capital, Karyopharm. Research Funding to Institution: BMS, Novartis, Merck, Genentech, GSK. JMK declares the following unrelated advisory activities and funding: Advisory Role: Bristol Myers Squibb, Novartis, lovance Biotherapeutics, Elsevier, Amgen, Checkmate Pharmaceuticals, Harbour BioMed, Istari Oncology, OncoSec, Scopus BioPharma, Pfizer; Speakers' Bureau: Bristol Myers Squibb unbranded IO; Research Funding: Amgen, Bristol Myers Squibb, Castle Biosciences, Checkmate Pharmaceuticals, Immunocore, lovance Biotherapeutics, Novartis, Merck.

Patient consent for publication Not applicable.

Ethics approval The study was conducted per Declaration of Helsinki principles. Approval to treat patients was obtained from the University of Pittsburgh Cancer Institute (UPCI)/Hillman Cancer Center (HCC) Institutional Review Board (No. PR012060479). The authors attest that signed informed consent was obtained from all patients entered onto this study.

Provenance and peer review Not commissioned; externally peer reviewed.

Data availability statement Data are available upon reasonable request. The full trial protocol and all data relevant to the study will be provided upon reasonable request.

Supplemental material This content has been supplied by the author(s). It has not been vetted by BMJ Publishing Group Limited (BMJ) and may not have been peer-reviewed. Any opinions or recommendations discussed are solely those of the author(s) and are not endorsed by BMJ. BMJ disclaims all liability and

responsibility arising from any reliance placed on the content. Where the content includes any translated material, BMJ does not warrant the accuracy and reliability of the translations (including but not limited to local regulations, clinical guidelines, terminology, drug names and drug dosages), and is not responsible for any error and/or omissions arising from translation and adaptation or otherwise.

Open access This is an open access article distributed in accordance with the Creative Commons Attribution Non Commercial (CC BY-NC 4.0) license, which permits others to distribute, remix, adapt, build upon this work non-commercially, and license their derivative works on different terms, provided the original work is properly cited, appropriate credit is given, any changes made indicated, and the use is non-commercial. See <http://creativecommons.org/licenses/by-nc/4.0/>.

ORCID iDs

Walter J Storkus <http://orcid.org/0000-0001-8961-4444>
 Geoffrey M Lowman <http://orcid.org/0000-0002-1498-4165>
 Lisa H Butterfield <http://orcid.org/0000-0002-3439-9844>
 Ahmad Tarhini <http://orcid.org/0000-0002-3193-9702>
 Hussein Tawbi <http://orcid.org/0000-0003-1942-851X>

REFERENCES

- 1 Cancer Facts and Figures 2020. American Cancer Society, Atlanta, GA, USA, 2021. Available: <https://www.cancer.org/content/dam/cancer-org/research/cancer-facts-and-statistics/annual-cancer-facts-and-figures/2021/cancer-facts-and-figures-2021.pdf>
- 2 Balch CM, Gershenwald JE, Soong S-jaw, *et al.* Final version of 2009 AJCC melanoma staging and classification. *JCO* 2009;27:6199–206.
- 3 Linardou H, Gogas H. Toxicity management of immunotherapy for patients with metastatic melanoma. *Ann Transl Med* 2016;4:272.
- 4 Ascierto ML, Melero I, Ascierto PA. Melanoma: from incurable beast to a curable BET. The success of immunotherapy. *Front Oncol* 2015;5:152.
- 5 Melero I, Gaudernack G, Gerritsen W, *et al.* Therapeutic vaccines for cancer: an overview of clinical trials. *Nat Rev Clin Oncol* 2014;11:509–24.
- 6 Chi M, Dudek AZ. Vaccine therapy for metastatic melanoma: systematic review and meta-analysis of clinical trials. *Melanoma Res* 2011;21:165–74.
- 7 Zhang Y, Ertl HCJ. Starved and asphyxiated: How can CD8⁺ T cells within a tumor microenvironment prevent tumor progression. *Front Immunol* 2016;7:32.
- 8 Zhao X, Bose A, Komita H, *et al.* Vaccines targeting tumor blood vessel antigens promote CD8⁺ T cell-dependent tumor eradication or dormancy in HLA-A2 transgenic mice. *J Immunol* 2012;188:1782–8.
- 9 Chi Sabins N, Taylor JL, Fabian KPL, *et al.* DLK1: a novel target for immunotherapeutic remodeling of the tumor blood vasculature. *Mol Ther* 2013;21:1958–68.
- 10 Komita H, Zhao X, Taylor JL, *et al.* CD8⁺ T-cell responses against hemoglobin-beta prevent solid tumor growth. *Cancer Res* 2008;68:8076–84.
- 11 Kluger HM, Dudek AZ, McCann C, *et al.* A phase 2 trial of dasatinib in advanced melanoma. *Cancer* 2011;117:2202–8.
- 12 Lowe DB, Bose A, Taylor JL, *et al.* Dasatinib promotes the expansion of a therapeutically superior T-cell repertoire in response to dendritic cell vaccination against melanoma. *Oncoimmunology* 2014;3:e27589.
- 13 Song N, Guo H, Ren J. Synergistic anti-tumor effects of dasatinib and dendritic cell vaccine on metastatic breast cancer in a mouse model. *Oncol Lett* 2018;15:6831–8.
- 14 Mailliard RB, Wankowicz-Kalinska A, Cai Q, *et al.* alpha-type-1 polarized dendritic cells: a novel immunization tool with optimized CTL-inducing activity. *Cancer Res* 2004;64:5934–7.
- 15 Butterfield LH, Vujanovic L, Santos PM, *et al.* Multiple antigen-engineered DC vaccines with or without IFN α to promote antitumor immunity in melanoma. *J Immunother Cancer* 2019;7:113.
- 16 Brossart P. The role of antigen spreading in the efficacy of immunotherapies. *Clin Cancer Res* 2020;26:4442–7.
- 17 Postow MA, Manuel M, Wong P, *et al.* Peripheral T cell receptor diversity is associated with clinical outcomes following ipilimumab treatment in metastatic melanoma. *J Immunother Cancer* 2015;3:23.
- 18 Looney TJ, Topacio-Hall D, Lowman G, *et al.* TCR convergence in individuals treated with immune checkpoint inhibition for cancer. *Front Immunol* 2019;10:2985.
- 19 Giallongo C, Parrinello NL, La Cava P, *et al.* Monocytic myeloid-derived suppressor cells as prognostic factor in chronic myeloid leukaemia patients treated with dasatinib. *J Cell Mol Med* 2018;22:1070–80.

- 20 Najima Y, Yoshida C, Iriyama N, *et al.* Regulatory T cell inhibition by dasatinib is associated with natural killer cell differentiation and a favorable molecular response-The final results of the D-first study. *Leuk Res* 2018;66:66–72.
- 21 Mohty A-M, Grob J-J, Mohty M, *et al.* Induction of IP-10/CXCL10 secretion as an immunomodulatory effect of low-dose adjuvant interferon-alpha during treatment of melanoma. *Immunobiology* 2010;215:113–23.
- 22 Zhou J, Mahoney KM, Giobbie-Hurder A, *et al.* Soluble PD-L1 as a biomarker in malignant melanoma treated with checkpoint blockade. *Cancer Immunol Res* 2017;5:480–92.
- 23 Winkler CA, Kittelberger AM, Schwartz GJ. Expression of carbonic anhydrase IV mRNA in rabbit kidney: stimulation by metabolic acidosis. *Am J Physiol* 1997;272:F551–60.
- 24 Cabrera R, Lauss M, Sanna A, *et al.* Tertiary lymphoid structures improve immunotherapy and survival in melanoma. *Nature* 2020;577:561–5.
- 25 Helmink BA, Reddy SM, Gao J, *et al.* B cells and tertiary lymphoid structures promote immunotherapy response. *Nature* 2020;577:549–55.
- 26 Petitprez F, de Reyniès A, Keung EZ, *et al.* B cells are associated with survival and immunotherapy response in sarcoma. *Nature* 2020;577:556–60.
- 27 Kalinsky K, Lee S, Rubin KM, *et al.* A phase 2 trial of dasatinib in patients with locally advanced or stage IV mucosal, acral, or vulvovaginal melanoma: a trial of the ECOG-ACRIN cancer research Group (E2607). *Cancer* 2017;123:2688–97.
- 28 Kluger HM, Dudek AZ, McCann C, *et al.* A phase 2 trial of dasatinib in advanced melanoma. *Cancer* 2011;117:2202–8.
- 29 Bol KF, Schreiber G, Gerritsen WR, *et al.* Dendritic cell-based immunotherapy: state of the art and beyond. *Clin Cancer Res* 2016;22:1897–906.
- 30 Banchereau J, Palucka AK, Dhodapkar M, *et al.* Immune and clinical responses in patients with metastatic melanoma to CD34(+) progenitor-derived dendritic cell vaccine. *Cancer Res* 2001;61:6451–8.
- 31 Butterfield LH, Comin-Anduix B, Vujanovic L, *et al.* Adenovirus MART-1-engineered autologous dendritic cell vaccine for metastatic melanoma. *J Immunother* 2008;31:294–309.
- 32 Butterfield LH, Ribas A, Dissette VB, *et al.* Determinant spreading associated with clinical response in dendritic cell-based immunotherapy for malignant melanoma. *Clin Cancer Res* 2003;9:998–1008.
- 33 Butterfield LH, Ribas A, Dissette VB, *et al.* A phase I/II trial testing immunization of hepatocellular carcinoma patients with dendritic cells pulsed with four alpha-fetoprotein peptides. *Clin Cancer Res* 2006;12:2817–25.
- 34 Song N, Guo H, Ren J, *et al.* Synergistic anti-tumor effects of dasatinib and dendritic cell vaccine on metastatic breast cancer in a mouse model. *Oncol Lett* 2018;15:6831–8.
- 35 Climent N, Plana M. Immunomodulatory activity of tyrosine kinase inhibitors to elicit cytotoxicity against cancer and viral infection. *Front Pharmacol* 2019;10:1232.
- 36 Chu C-L, Lee Y-P, Pang C-Y, *et al.* Tyrosine kinase inhibitors modulate dendritic cell activity via confining c-Kit signaling and tryptophan metabolism. *Int Immunopharmacol* 2020;82:106357.
- 37 Boltjes A, van Wijk F. Human dendritic cell functional specialization in steady-state and inflammation. *Front Immunol* 2014;5:131.
- 38 Mestermann K, Giavridis T, Weber J, *et al.* The tyrosine kinase inhibitor dasatinib acts as a pharmacologic on/off switch for CAR T cells. *Sci Transl Med* 2019;11:eaa5907.
- 39 Furman D. Sexual dimorphism in immunity: improving our understanding of vaccine immune responses in men. *Expert Rev Vaccines* 2015;14:461–71.
- 40 Trigunaite A, Dimo J, Jørgensen TN. Suppressive effects of androgens on the immune system. *Cell Immunol* 2015;294:87–94.
- 41 Gold SM, Willing A, Leyboldt F, *et al.* Sex differences in autoimmune disorders of the central nervous system. *Semin Immunopathol* 2019;41:177–88.
- 42 Lin P-Y, Sun L, Thibodeaux SR, *et al.* B7-H1-dependent sex-related differences in tumor immunity and immunotherapy responses. *J Immunol* 2010;185:2747–53.
- 43 Capone I, Marchetti P, Ascierto PA, *et al.* Sexual dimorphism of immune responses: a new perspective in cancer immunotherapy. *Front Immunol* 2018;9:552.
- 44 Loo K, Tsai KK, Mahuron K, *et al.* Partially exhausted tumor-infiltrating lymphocytes predict response to combination immunotherapy. *JCI Insight* 2017;2:93433.
- 45 Gopalakrishnan V, Helmink BA, Spencer CN, *et al.* The influence of the gut microbiome on cancer, immunity, and cancer immunotherapy. *Cancer Cell* 2018;33:570–80.
- 46 Gomez A, Luckey D, Taneja V. The gut microbiome in autoimmunity: sex matters. *Clin Immunol* 2015;159:154–62.
- 47 Motzer RJ, Escudier B, McDermott DF, *et al.* Nivolumab versus everolimus in advanced renal-cell carcinoma. *N Engl J Med* 2015;373:1803–13.
- 48 Robert C, Long GV, Brady B, *et al.* Nivolumab in previously untreated melanoma without BRAF mutation. *N Engl J Med* 2015;372:320–30.
- 49 Botticelli A, Onesti CE, Zizzari I, *et al.* The sexist behaviour of immune checkpoint inhibitors in cancer therapy? *Oncotarget* 2017;8:99336–46.
- 50 Heidari S, Babor TF, De Castro P, *et al.* Sex and gender equity in research: rationale for the SAGER guidelines and recommended use. *Res Integr Peer Rev* 2016;1:2.
- 51 Rossi E, Schinzari G, Maiorano BA, *et al.* Efficacy of immune checkpoint inhibitors in different types of melanoma. *Hum Vaccin Immunother* 2021;17:4–13.
- 52 Ott PA, Hu-Lieskovan S, Chmielowski B, *et al.* A phase Ib trial of personalized neoantigen therapy plus anti-PD-1 in patients with advanced melanoma, non-small cell lung cancer, or bladder cancer. *Cell* 2020;183:347–62.
- 53 Lai J, Mardiana S, House IG, *et al.* Adoptive cellular therapy with T cells expressing the dendritic cell growth factor Flt3L drives epitope spreading and antitumor immunity. *Nat Immunol* 2020;21:914–26.
- 54 Charles J, Mouret S, Challengé I, *et al.* T-cell receptor diversity as a prognostic biomarker in melanoma patients. *Pigment Cell Melanoma Res* 2020;33:612–24.
- 55 Naidus E, Bouquet J, Oh DY, *et al.* Early changes in the circulating T cells are associated with clinical outcomes after PD-L1 blockade by durvalumab in advanced NSCLC patients. *Cancer Immunol Immunother* 2021;70:2095–102.
- 56 Maurer DM, Adamik J, Santos PM, *et al.* Dysregulated NF-κB-dependent ICOSL expression in human dendritic cell vaccines impairs T-cell responses in patients with melanoma. *Cancer Immunol Res* 2020;8:1554–67.
- 57 Marinelaarena A, Bhattacharya P, Kumar P, *et al.* Identification of a Novel OX40L⁺ Dendritic Cell Subset That Selectively Expands Regulatory T cells. *Sci Rep* 2018;8:14940.
- 58 Asporid C, Leccia M-T, Charles J, *et al.* Plasmacytoid dendritic cells support melanoma progression by promoting Th2 and regulatory immunity through OX40L and ICOSL. *Cancer Immunol Res* 2013;1:402–15.
- 59 Chapoval AI, Smithson G, Brunick L, *et al.* BTN1L, a butyrophilin-like molecule that costimulates the primary immune response. *Mol Immunol* 2013;56:819–28.
- 60 Ueno Y, Fujisaki K, Hosoda S, *et al.* Transcription factor Tlx1 marks a subset of lymphoid tissue organizer-like mesenchymal progenitor cells in the neonatal spleen. *Sci Rep* 2019;9:20408.
- 61 Tesone AJ, Rutkowski MR, Brencicova E, *et al.* Satb1 overexpression drives tumor-promoting activities in cancer-associated dendritic cells. *Cell Rep* 2016;14:1774–86.
- 62 Carvalheiro T, Garcia S, Pascoal Ramos MI, *et al.* Leukocyte associated immunoglobulin like receptor 1 regulation and function on monocytes and dendritic cells during inflammation. *Front Immunol* 2020;11:11.
- 63 Lin H, Wei S, Hurt EM, *et al.* Host expression of PD-L1 determines efficacy of PD-L1 pathway blockade-mediated tumor regression. *J Clin Invest* 2018;128:805–15.
- 64 Li X, Gong L, Gu H. Regulation of immune system development and function by Cbl-mediated ubiquitination. *Immunol Rev* 2019;291:123–33.
- 65 Okabe S, Tauchi T, Ohyashiki K, *et al.* Stromal-cell-derived factor-1/CXCL12-induced chemotaxis of a T cell line involves intracellular signaling through Cbl and Cbl-b and their regulation by Src kinases and CD45. *Blood Cells Mol Dis* 2006;36:308–14.
- 66 Li J, Jie H-B, Lei Y, *et al.* PD-1/SHP-2 inhibits Tc1/Th1 phenotypic responses and the activation of T cells in the tumor microenvironment. *Cancer Res* 2015;75:508–18.
- 67 Lanier LL. NK cell receptors. *Annu Rev Immunol* 1998;16:359–93.
- 68 Villarreal DO, Wise MC, Siefert RJ, *et al.* Ubiquitin-like molecule ISG15 acts as an immune adjuvant to enhance antigen-specific CD8 T-cell tumor immunity. *Mol Ther* 2015;23:1653–62.
- 69 Wood LM, Pan Z-K, Seavey MM, *et al.* The ubiquitin-like protein, ISG15, is a novel tumor-associated antigen for cancer immunotherapy. *Cancer Immunol Immunother* 2012;61:689–700.
- 70 Chen R-H, Xiao Z-W, Yan X-Q, *et al.* Tumor cell-secreted ISG15 promotes tumor cell migration and immune suppression by inducing the macrophage M2-like phenotype. *Front Immunol* 2020;11:594775.

Table S1. Patient Demographics and Clinical Characteristics (n = 15)

Characteristic	Arm A (n = 9)	Arm B (n= 6)	All (n = 15)
Median age, years (range)*	70 (44-75)	65 (42-84)	70 (42-84)
Sex			
Male	5	3	8
Female	4	3	7
Caucasian Ethnicity	9	6	15
Disease Stage			
N/A	1	0	1
Stage IIC	0	1	1
Stage IV	8	5	13
ECOG performance status			
0	3	2	5
1	5	4	9
2	1	0	1
Primary melanoma site			
Skin	4	5	9
Eye	4	1	5
Mucosa	1	0	1
Extent of disease			
LN metastases (any site)	4	4	8
Lung metastases	5	4	9
Liver metastases	5	2	7
Non-lung/liver mets	6	4	10
BMI, median (range)*	28.4 (24.8-32.4)	28.9 (24.2-47.9)	28.4 (24.2-47.9)
BSA, g/dl median (range)*	1.92 (1.67-2.21)	1.98 (1.84-2.53)	1.92 (1.67-2.53)
LDH level, IU/L median (range)*	303.5 (140-1867)	199.5 (151-214)	213.0 (140-1867)
Prior immunomodulatory therapy			
IL-2	1	2	3
IFN α	3	1	4
Anti-CTLA4 monotherapy	7	2	9
Anti-PD1 monotherapy	8	4	12
Anti-CTLA4/PD1 combined	1	1	2
Vaccines**	3	1	4
Number of prior therapies***			
0	0	0	0
1	0	1	1
2	3	2	5
≥ 3	6	3	9

Abbreviations: CTLA4, cytotoxic T-lymphocyte-associated protein 4; ECOG, Eastern Cooperative Oncology Group; IFN, interferon; LN, lymph node; PD1, programmed death-1.

*NS for Arm A vs. Arm B; **UPCI 09-021/NCT01622933 (vaccination with autologous DC infected with a recombinant adenovirus encoding the MAGE-6, MART1 and tyrosinase antigens); ***Includes chemotherapy, immunotherapy, radiotherapy and surgery.

Storkus et al.

Table S2. Best Response to Treatment in Evaluable Patients (n = 13)

Response	Arm A (n = 7)	Arm B (n = 6)	All (n = 13)
CD8 ⁺ T cell Response (Vaccine)*	2	4	6
OCR (best RECIST1.1)			
Complete response	0	0	0
Partial response	0	4	4
Stable disease	3	0	3
Progressive disease	4	2	6
OCR Response Rate	0.0000	0.6667	0.3077
OS median months (range)**	8.3 (3.0-19.6)	19.1 (9.1-28.4)	15.2 (3.0-28.4)
PFS median months (range)***	2.2 (1.9-9.7)	7.9 (2.1-25.3)	4.2 (1.9-25.3)

* Positive response to ≥ 3 vaccine peptides in IFN- γ ELISPOT assays.

** p = 0.0086 for Arm B vs. Arm A.

*** p = 0.063 for Arm B vs. Arm A.

Abbreviations: OCR, objective clinical response; OS, overall survival; PFS, progression-free survival.

Table S3. Summary of Adverse Events (AEs)

AE Grade	Number of Patients with Indicated AE Grade Events:		
	Arm A (n = 9)	Arm B (n = 6)	Total (n = 15)
2	4 [44%]	3 [50%]	3 [47%]
3	1 [11%]	2 [33%]	3 [20%]
N/A	1* [11%]	0 [0%]	1* [11%]

*Lymphoma diagnosis unrelated to treatment in patient #11.

Table S4. Patient AEs by Category (n = 15).

Toxicity	Arm A				Arm B			
	Grade 1-2	%	Grade 3	%	Grade 1-2	%	Grade 3	%
Abdominal pain	0	0	1	11.11	1	16.67	0	0
Acute kidney injury	1	11.11	0	0	0	0	0	0
Alkaline phosphatase increased	2	22.22	0	0	1	16.67	0	0
Anemia	5	55.56	1	11.11	3	50	2	33.33
Anorexia	2	22.22	0	0	2	33.33	0	0
Arthralgia	0	0	0	0	0	0	1	16.67
Aspartate aminotransferase increased	2	22.22	0	0	2	33.33	0	0
Bruising	0	0	0	0	1	16.67	0	0
Cardiac disorders - Other, specify	0	0	0	0	0	0	1	16.67
Chills	1	11.11	0	0	1	16.67	0	0
Cough	1	11.11	0	0	0	0	0	0
Creatinine increased	0	0	0	0	1	16.67	0	0
Diarrhea	1	11.11	0	0	2	33.33	0	0
Dry skin	0	0	0	0	2	33.33	0	0
Dyspepsia	0	0	0	0	1	16.67	0	0
Erythema multiforme	0	0	0	0	1	16.67	0	0
Fatigue	5	55.56	1	11.11	5	83.33	0	0
Fever	0	0	0	0	2	33.33	0	0
Gastrointestinal disorders - Other, specify	0	0	0	0	1	16.67	0	0
General disorders and administration site conditions - Other, specify	0	0	0	0	1	16.67	0	0
Generalized muscle weakness	1	11.11	0	0	0	0	0	0
Headache	0	0	0	0	2	33.33	0	0
Hypermagnesemia	0	0	0	0	1	16.67	0	0
Hypoalbuminemia	2	22.22	0	0	1	16.67	0	0
Hypocalcemia	2	22.22	0	0	1	16.67	0	0
Hypokalemia	1	11.11	0	0	2	33.33	0	0

Storkus et al.

Hypomagnesemia	1	11.11	0	0	0	0	0	0
Hyponatremia	4	44.44	0	0	5	83.33	0	0
Hypoparathyroidism	0	0	0	0	1	16.67	0	0
Hypophosphatemia	2	22.22	0	0	3	50	1	16.67
Hypotension	0	0	0	0	1	16.67	0	0
Hypothyroidism	0	0	0	0	1	16.67	0	0
Insomnia	0	0	0	0	1	16.67	0	0
Investigations - Other, specify	1	11.11	0	0	1	16.67	0	0
Leukocytosis	0	0	0	0	1	16.67	0	0
Lymphedema	1	11.11	0	0	0	0	0	0
Lymphocyte count decreased	2	22.22	2	22.22	0	0	0	0
Lymphocyte count increased	0	0	0	0	3	50	0	0
Metabolism and nutrition disorders - Other, specify	1	11.11	0	0	1	16.67	0	0
Myalgia	0	0	0	0	0	0	1	16.67
Nausea	1	11.11	0	0	5	83.33	0	0
Neutrophil count decreased	2	22.22	0	0	4	66.67	0	0
Pain	0	0	0	0	1	16.67	0	0
Pain in extremity	0	0	0	0	1	16.67	0	0
Phlebitis infective	0	0	0	0	1	16.67	0	0
Platelet count decreased	2	22.22	0	0	3	50	0	0
Productive cough	0	0	0	0	1	16.67	0	0
Pruritus	0	0	0	0	1	16.67	0	0
Rash maculopapular	0	0	1	11.11	3	50	0	0
Skin and subcutaneous tissue disorders - Other, specify	1	11.11	0	0	2	33.33	0	0
Uterine hemorrhage	0	0	0	0	1	16.67	0	0
Vomiting	0	0	0	0	4	66.67	0	0
Weight loss	1	11.11	0	0	1	16.67	0	0
White blood cell decreased	1	11.11	0	0	2	33.33	0	0

Storkus et al.

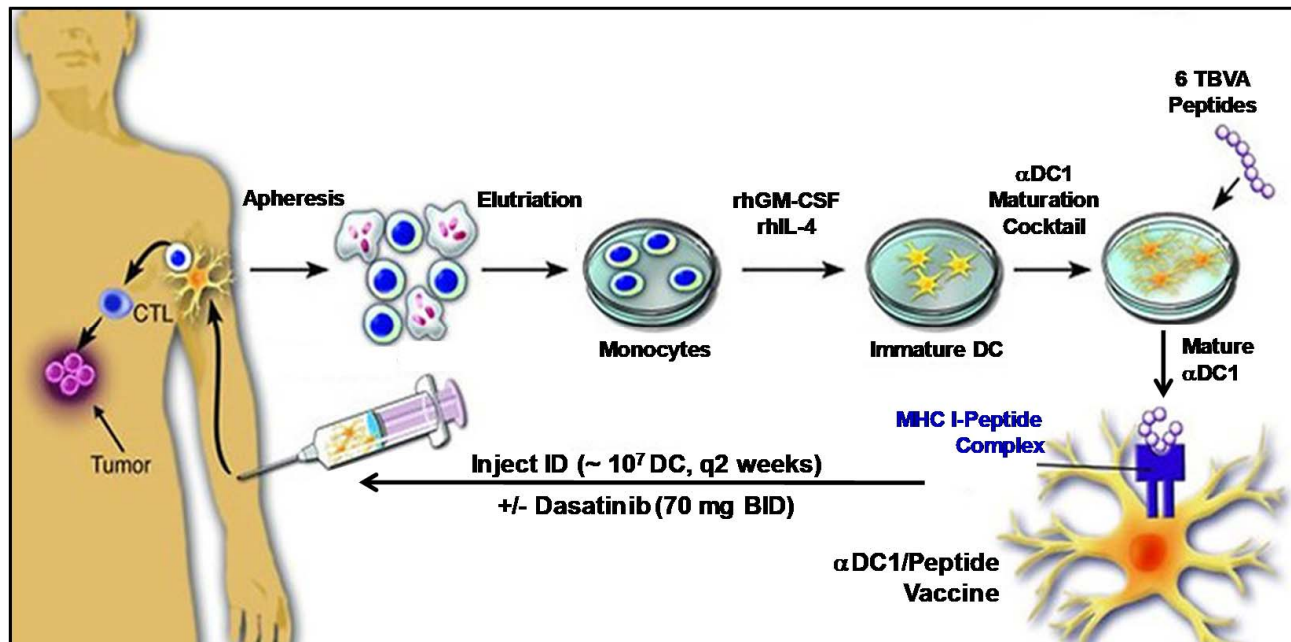


Fig. S1. Generation of autologous α DC1/TBVA peptide-based vaccines and use in NCT01876212. Patient monocytes elutriated from apheresis products were cultured in the presence of rhGM-CSF + rhIL-4 for 5 days to generate immature DC, which were then matured into α DC1 and loaded with a mixture of 6 HLA-A2-binding peptides derived from TBVA as outlined in Materials and Methods. Approximately 10⁷ TBVA peptide-loaded α DC1 were injected i.d. every 2 weeks in the vicinity of the nodal drainage groups of the four extremities. Dasatinib was administered (70 mg p.o. BID) beginning in either week 1 (Arm B) or week 5 (Arm A). Based on our therapeutic paradigm, injected peptide-loaded α DC1 initiate the cross-priming of antigen-specific CD8⁺ T (CTL) cell responses that are competent to target the tumor-associated vasculature, infiltrate the TME and mediate anti-tumor therapeutic activity in effectively vaccinated patients.

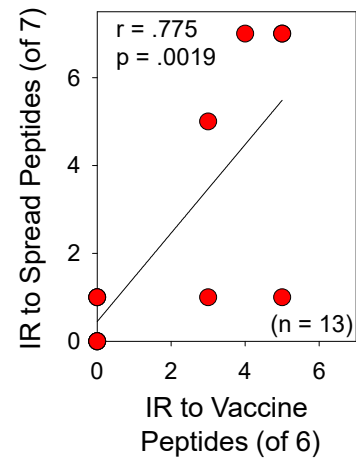


Figure S2. Patient immune response (IR) to vaccine peptides correlates with IR to spread (non-vaccine) peptides. The number of vaccine or non-vaccine peptides to which individual patients developed a positive response on-treatment (per Fig. 2A) was determined using IFN- γ ELISPOT assays as outlined in Materials and Methods.

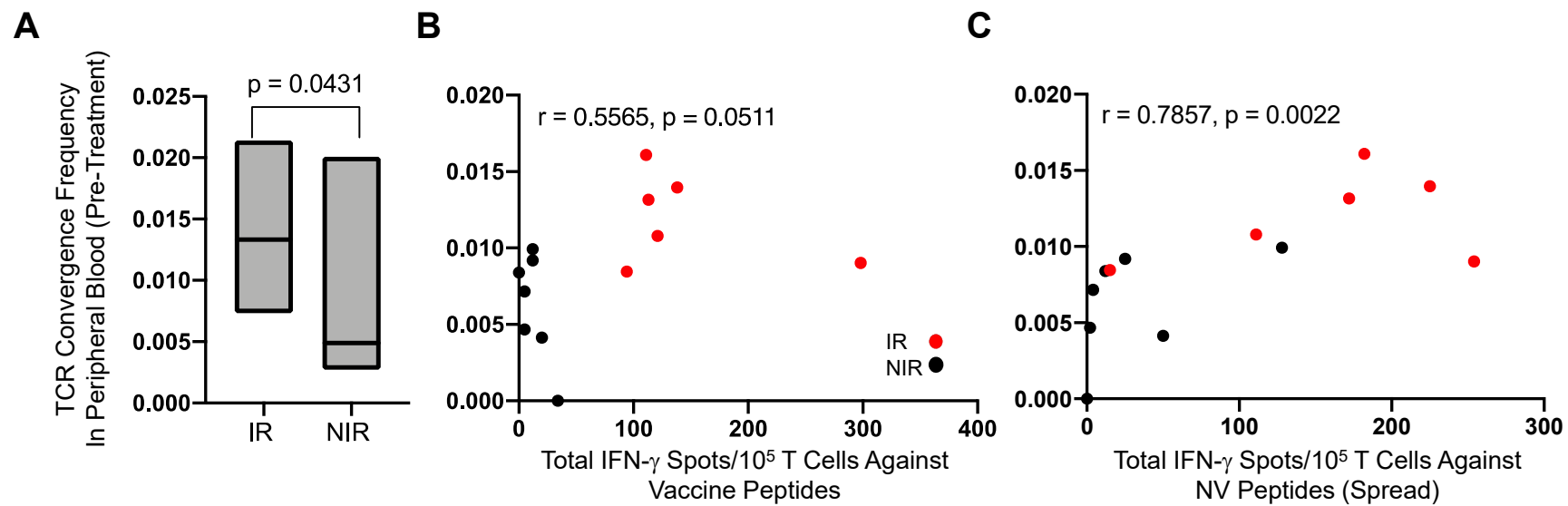


Figure S3. Peripheral blood TCR convergence at baseline is associated with patient response to vaccine peptides and epitope spreading (ES). In **A**, patient baseline peripheral blood TCR convergence is reported based on patient immune response (IR) to vaccine peptides vs. no immune response (NIR) to vaccine peptides. TCR convergence is plotted vs. cumulative T cell response to vaccine (**B**) or non-vaccine (NV) peptides (**C**) as determined in IFN- γ ELISPOT assays, with the latter serving as an index of epitope spreading in the patient T cell repertoire on-treatment.

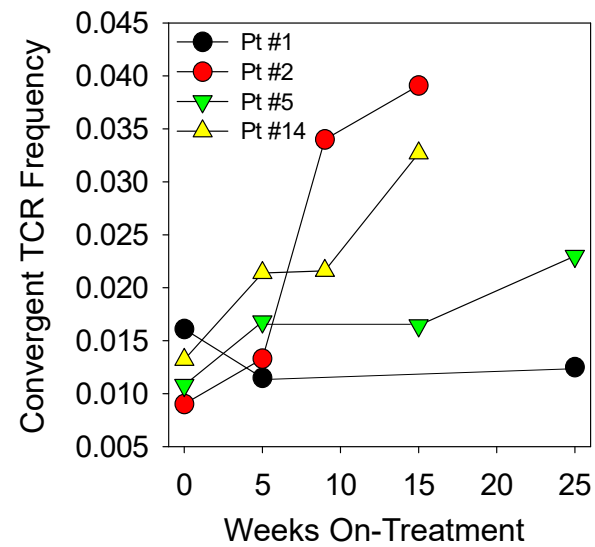


Figure S4. TCR convergence in the peripheral blood T cell repertoire remains stable or increases over time on-treatment in PR patients. Peripheral blood specimens isolated from patients at baseline vs. the indicated time points on-treatment were analyzed using OncoPrint TCRB-LR assays for TCR convergence as described in Materials and Methods.

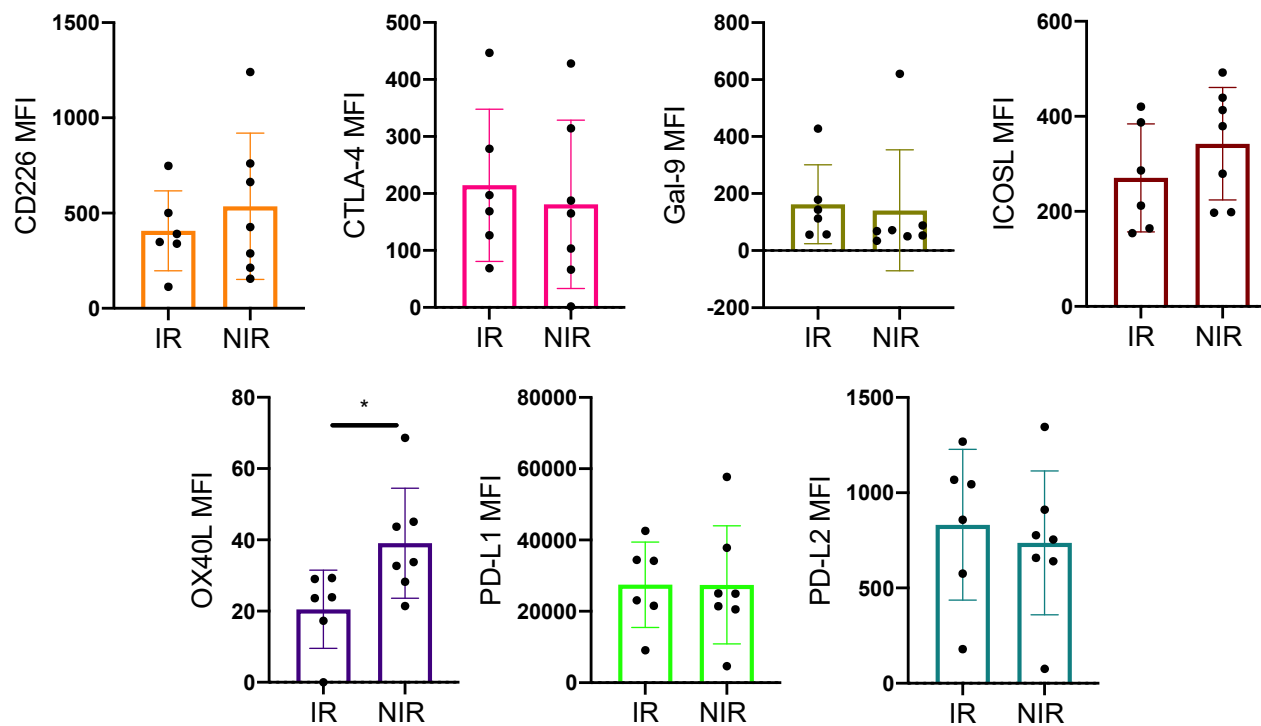


Figure S5. Flow cytometry analysis of cell surface costimulatory and checkpoint molecules on vaccine α DC1 segregated based on patient immunologic/clinical response to treatment. Aliquots of cryopreserved vaccine α DC1 were stained for the indicated cell surface proteins and analyzed by flow cytometry as outlined in Materials and Methods. Abbreviations: IR, immune response to vaccination; MFI, mean fluorescence intensity; NIR, no immunologic response to vaccination.

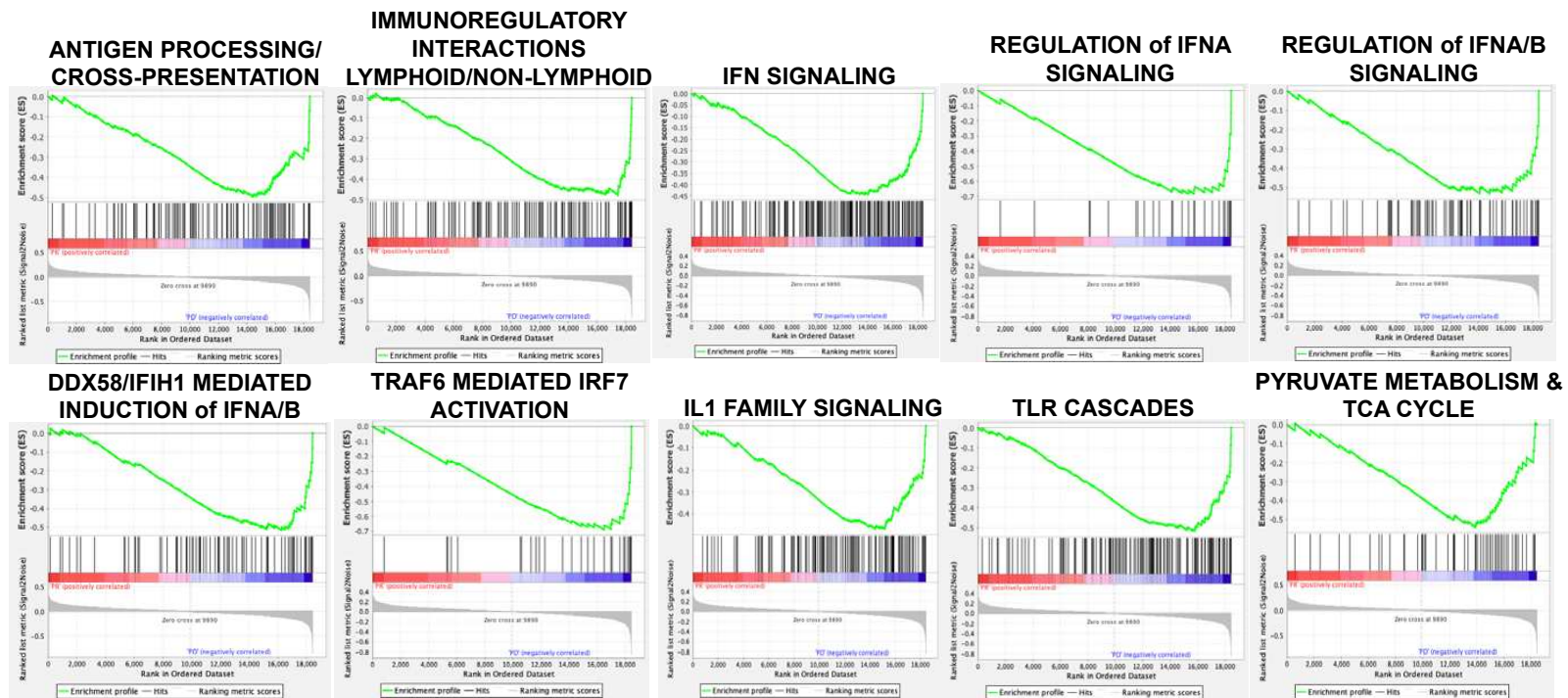


Figure S6. Predominance of gene signatures associated with deficiency in antigen-presenting cell function and IFN/TLR/IL1 family cytokine signaling in α DC1 from NIR/PD vs. IR/PR patients. Gene array profiling of patient vaccine α DC1 tumor biopsy tissues was performed as outlined in Fig. 4 and Materials and Methods, with gene set enrichment ($p < 0.05$) then assessed using GSEA software (V.4.1.0) as described in Supplemental Materials and Methods.

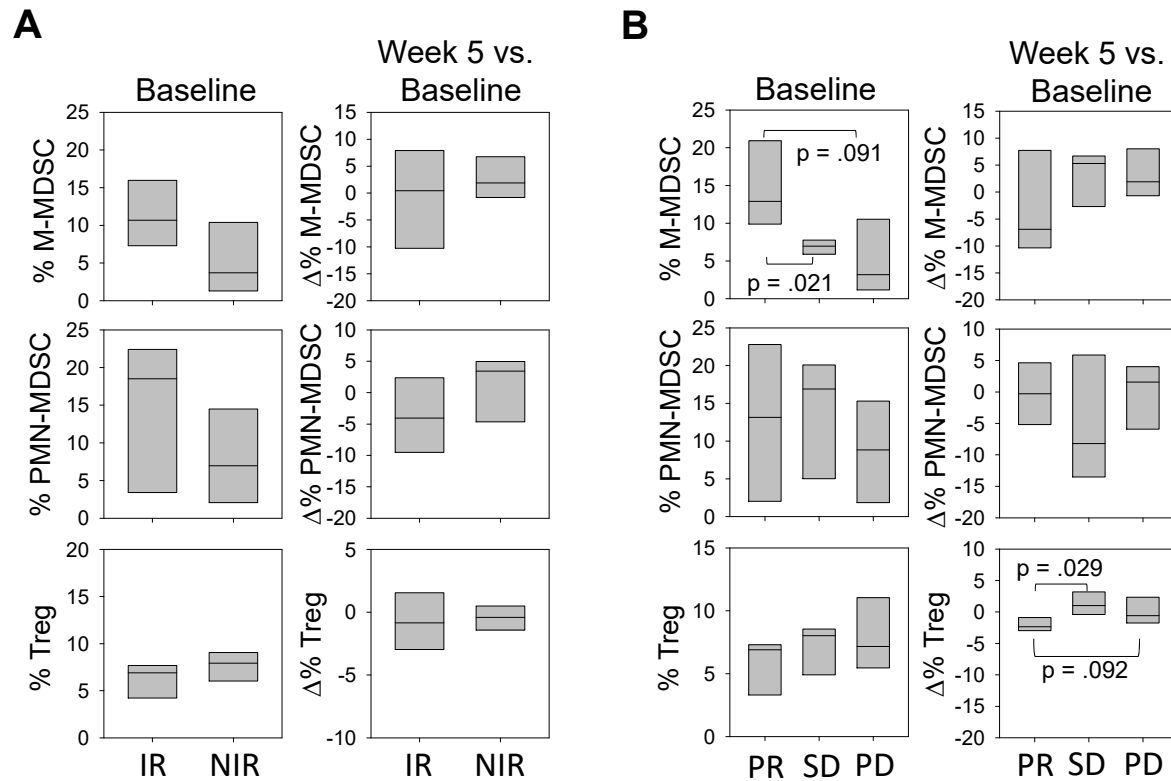


Figure S7. Peripheral blood regulatory cells exhibited modest changes in frequency on-treatment. Frequencies of myeloid-derived suppressor cells (M-MDSC and PMN-MDSC) and FoxP3⁺CD4⁺ Treg cells in patient peripheral blood were determined by flow cytometry at baseline and on-treatment (week 5 vs. baseline). Bar and whisker plots are provided based on the segregation of patients based on IR (panel **A**) or OCR (panel **B**) status. Abbreviations: IR, immune response to vaccination; NIR, no immune response to vaccination; PD, progressive disease; PR, partial response; SD, stable disease.

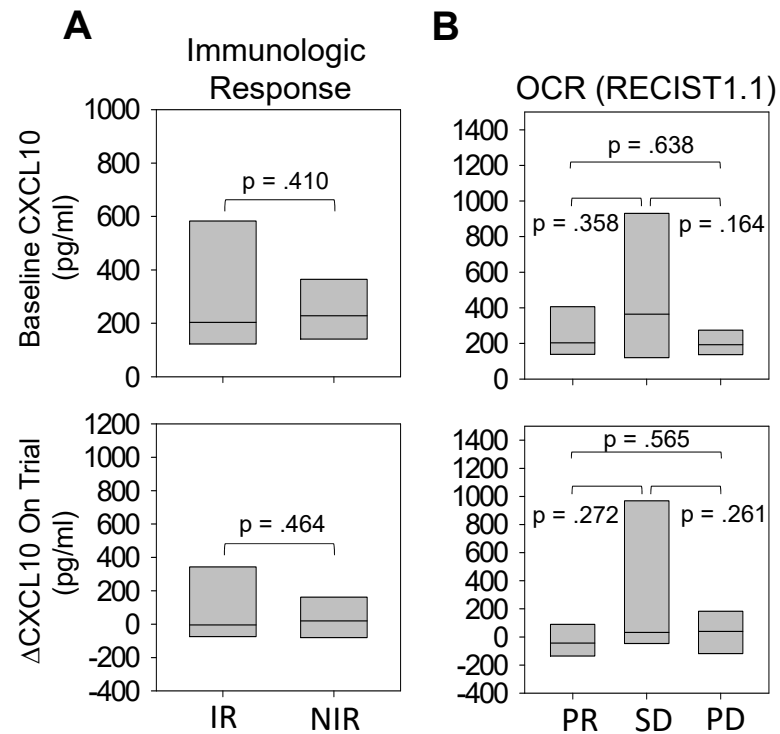


Figure S8. Serum CXCL10 fails to identify patients based on immune and clinical response to vaccination. Patient sera were isolated at baseline and 5 week on-treatment and analyzed for CXCL10 content by specific ELISA as outlined in Materials and Methods. Bar and whisker plots are depicted for patient results segregated based on (A) immune response (IR) vs non-immune response (NIR) to vaccine peptides as determined in IFN- γ ELISPOT assays or (B) OCR status on trial. Abbreviations: IR, immune response to vaccination; NIR, no immune response to vaccination; OCR, objective clinical response; PD, progressive disease; PR, partial response; SD, stable disease.

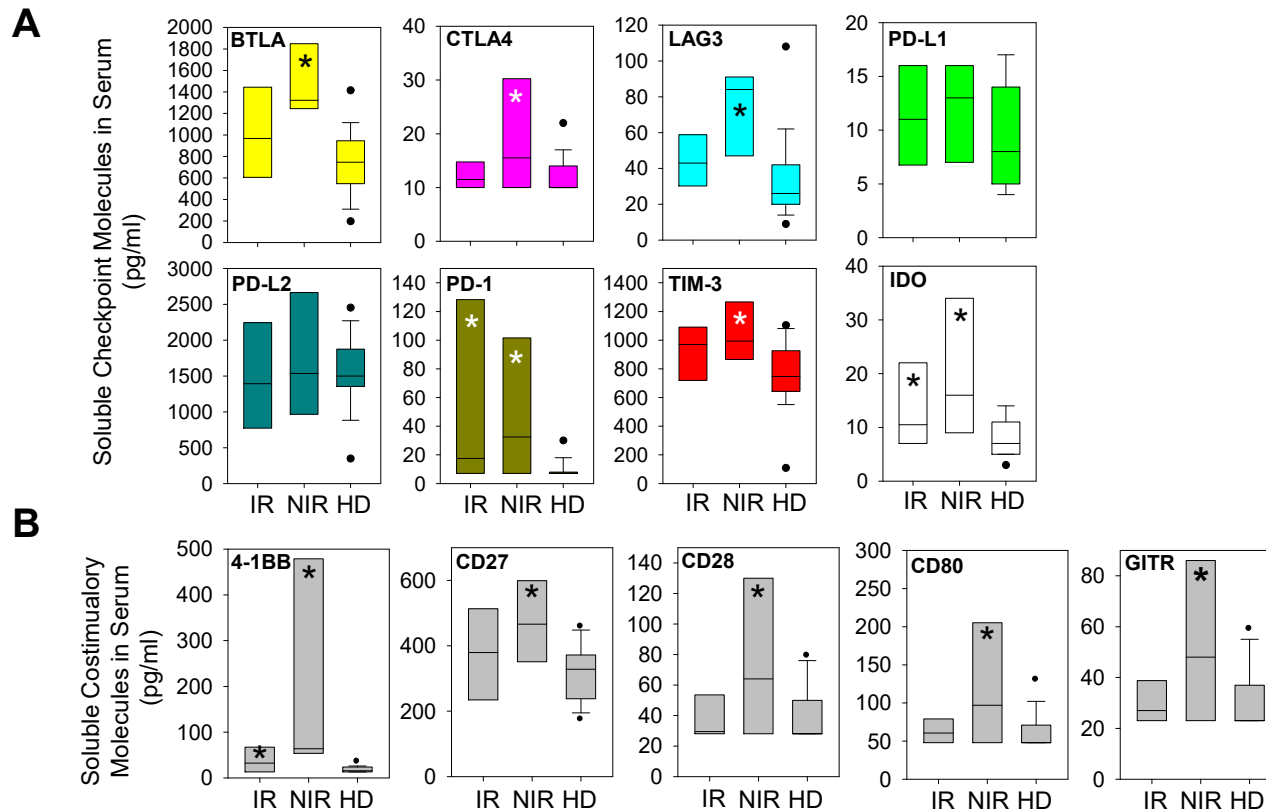


Figure S9. Serum levels of soluble checkpoint or costimulatory molecules fail to identify patients based on immune response to vaccination. Patient sera were isolated at baseline and 5 week on-treatment and analyzed for the indicated soluble checkpoint (A) or costimulatory (B) molecules using the multiplex Luminex Immuno-Oncology Checkpoint Marker Panel as described in Materials and Methods. Bar and whisker plots are depicted for patient results segregated based on immune response (IR) vs non-immune response (NIR) to vaccine peptides as determined in IFN- γ ELISPOT assays. Not significant (NS) for IR vs. NIR. * $p < 0.05$ vs. HD. Abbreviations: HD, healthy donors; IR, immune response to vaccination; NIR, no immune response to vaccination.

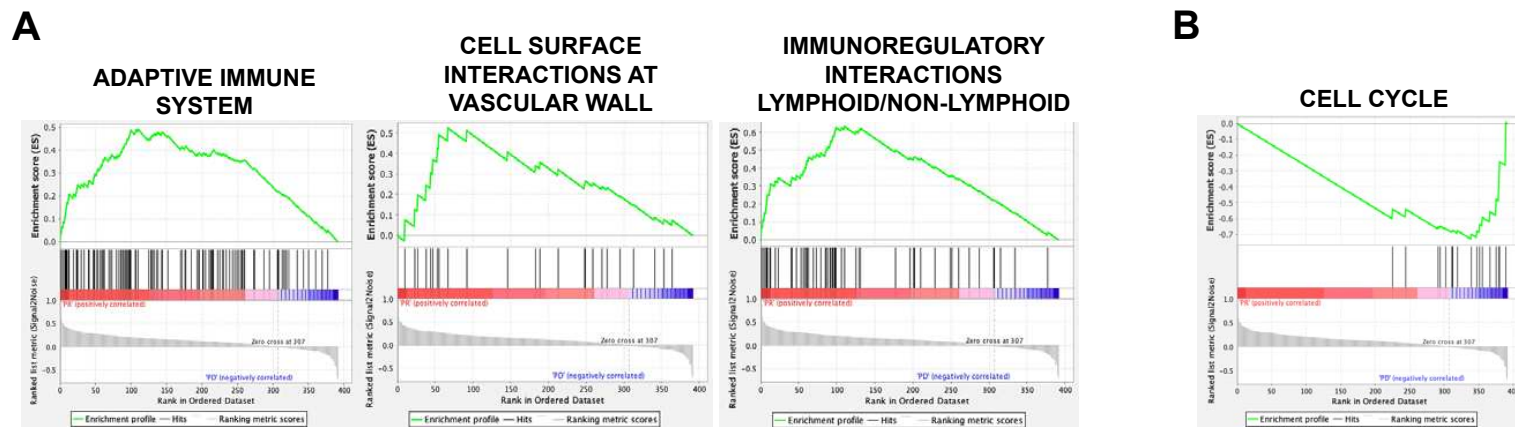


Figure S10. Baseline tumor pathways associated with patient outcomes on trial. OIRRA profiling of tumor biopsy tissues was performed as outlined in Fig. 5 and Materials and Methods, with gene set enrichment then performed using GSEA software (V.4.1.0) as described in Supplemental Materials and Methods. Baseline tumor pathways positively (A) or negatively (B) associated with PR/IR ($p < 0.05$).

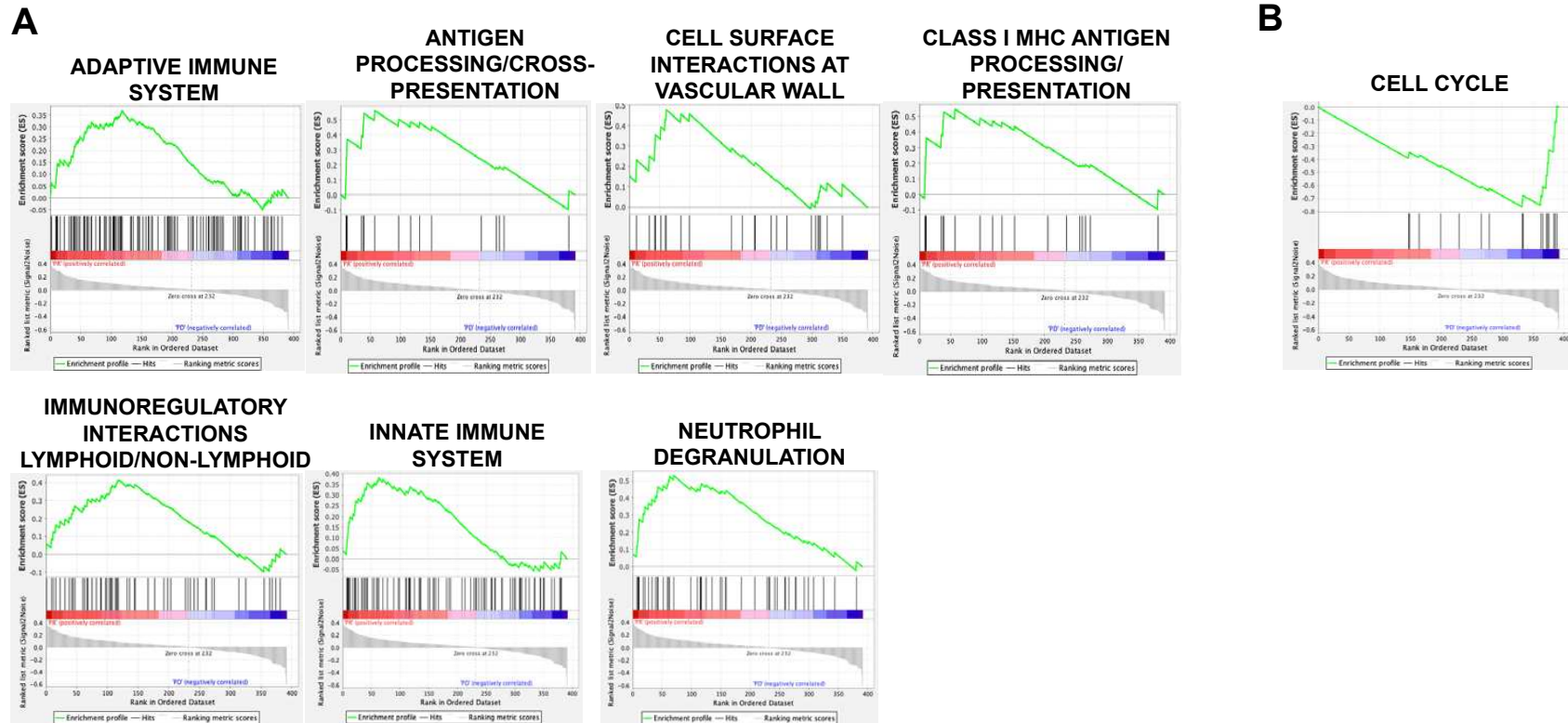


Figure S11. On-treatment tumor pathways associated with patient outcomes on trial. OIRRA profiling of tumor biopsy tissues was performed as outlined in Fig. 5 and Materials and Methods, with gene set enrichment then performed using GSEA software (V.4.1.0) as described in Supplemental Materials and Methods. On-treatment tumor pathways positively (A) or negatively (B) associated with PR/IR ($p < 0.05$).

SUPPLEMENTAL MATERIALS AND METHODS

Patient Eligibility

Eligible patients (≥ 18 years) had histologically confirmed, measurable disease by RECIST v1.1, with at least 2 tumor masses accessible for biopsy purposes, ECOG performance status < 2 , and a life expectancy of at least 12 weeks. Prior treatment with chemotherapy, immunotherapy or targeted therapy was allowed, if these treatments did not include dasatinib. Patients were excluded if they: i.) had received chemotherapy or radiotherapy within 4 weeks prior to entering the study, ii.) had not yet recovered from adverse events due to agents administered more than 4 weeks earlier, iii.) had documented c-KIT mutations, iv.) were receiving other investigational agents, v.) had active brain metastases, vi.) had a history of allergic reactions attributed to compounds of similar chemical or biologic composition to dasatinib or any of the components of the vaccine being administered, vii.) had a history of bleeding abnormalities or ventricular arrhythmias or viii.) had any active infection. The protocol was conducted per Declaration of Helsinki principles.

Patient Randomization and Assignment to Treatment Arm

Patients were randomized in a 1:1 ratio to the two study arms, stratified by BRAF mutation status. Patient randomization to treatment arm was conducted using the University of Pittsburgh Cancer Institute (UPCI) randomizer which was maintained by the Biostatistics Facility of the UPCI (<https://randomize.upci.pitt.edu/randomizer/home.seam>). The randomizer was accessed each time a new patient was enrolled, at which time only the assignment for that current patient was viewable. In all cases, the protocol coordinator (AR) assigned patients to interventions according to the randomizer's output.

Autologous α DC1/TBVA Peptide Vaccine Generation

Patients underwent a 3h apheresis procedure at baseline, for collection of a total volume of white blood cells between 125-250 ml. Vaccines were prepared according to cGMP guidance in the Immunologic Monitoring and Cellular Products Laboratory (IMCPL) at the Hillman Cancer Center. Elutriated leukapheresis product fractions enriched in monocytes were plated in DC medium (Cell Genix) with 1000 U/mL rhGM-CSF (Genzyme and Sanofi) and 1000 U/mL rhIL-4 (Cell Genix), with fresh cytokines added on day 3-4 of culture. On culture day 5, immature DC (iDC) were matured overnight by addition of clinical grade rhIL-1 β (10 ng/mL), rhTNF- α (10 ng/mL), rhIFN- α (3,000 U/mL), rhIFN- γ (1,000 U/ml), and poly-I:C (20 μ g/ml) at 37°C in 5% CO₂, as previously described^{S1}. Harvested mature α DC1 cells were then loaded with a cocktail of the certified

synthetic DLK1₃₁₀₋₃₁₈ (ILGVLTSLV), EphA2₈₈₃₋₈₉₁ (TLADFDPRV), HBB₃₁₋₃₉ (RLLVVYPWT), NRP1₄₃₃₋₄₄₁ (GMLGMVSGSL), RGS5₅₋₁₃ (LAALPHSCL), TEM1₆₉₁₋₇₀₀ (LLVPTCVFLV) peptides (at a final concentration of 1 µg/mL of each peptide in CellGenix media) for 3-4 hours at 37°C, 5% CO₂. Criteria for release of patient αDC1/peptide vaccines included: sterility by Gram stain and bacteriologic culture; negative *Mycoplasma*; endotoxin lower than 5.0 EU/kg of body weight; greater than 70% expression of both CD86 and HLA-DR on αDC1 cells as determined by flow cytometry. The first vaccine was administered fresh, with subsequent vaccines cryopreserved in 10% DMSO/40% AB serum/50% CellGenix medium until time of use when the cells were thawed prior to injection. Fresh and thawed vaccines were shown to be viable and phenotypically stable for at least 4h at 4°C. Freshly prepared patient αDC1 vaccine cells were also analyzed for secretion of IL-12p70 and IL-10 into culture supernatant after *in vitro* stimulation as previously described¹ using cytokine-specific ELISAs (BD Biosciences).

IFN_γ ELISPOT Assays

Patient peripheral blood T cell responses against peptides in the vaccine formulation were examined using standardized IFN_γ ELISPOT assays using HLA-A2⁺ T2 cells as an antigen-presenting cell. T2 cells were left untreated or pulsed with individual vaccine-associated TBVA peptides or HLA-A2-presented peptides derived from alternate TBVA-associated proteins (i.e. NRP1₃₃₁₋₃₃₉ [GLLRFTAV], PDGFRβ₈₉₀₋₈₉₈ [ILLWEIFTL], VEGFR1₇₇₀₋₇₇₈ [TLFWLLTL], VEGFR2₇₇₃₋₇₈₁ [VIAMFFWLL])^{S2,S3} or melanoma-associated proteins (i.e. MART1₂₆₋₃₅ [EAAGIGILTV], gp100₂₀₉₋₂₁₇ [ITDQVPFSV], TYR₃₆₈₋₃₇₆ [YMNGTMSQV])^{S4} overnight at 37°C, prior to washing in PBS and addition to IFN_γ ELISPOT wells. Triplicate determinations were performed. Plates were analyzed on a CTL Technologies ImmunoSpot reader (Cleveland, OH).

Flow Cytometry

Baseline and on-treatment patient peripheral blood mononuclear cells were analyzed for frequencies of CD4⁺Foxp3⁺ Treg, HLA-DR^{neg}CD3^{neg}CD11b⁺CD14⁺CD15^{neg}CD19^{neg}CD33⁺ monocytic MDSC (M-MDSC) and HLA-DR^{neg}CD3^{neg}CD11b⁺CD14^{neg}CD15⁺CD19^{neg}CD33⁺ polymorphonuclear MDSC (PMN-MDSC) using the following directly-conjugated antibody probes: α-FoxP3-PE antibody (eBioscience), α-HLA-DR-FITC (BD Pharmingen), α-CD3-PE-Cy7 (BD Pharmingen), α-CD4-FITC (BD Pharmingen), α-CD19-PE-Cy7 (BD Biosciences), α-CD33-APC (BD Pharmingen), α-CD11b-Pacblue (BD Pharmingen), α-CD14-PerCP (BD Biosciences), and α-CD15-PE (BD Pharmingen). Data analysis was performed using FACSDiva™ software (BD Biosciences). For Treg, cells were first stained using α-CD4 mAb, then washed and

fixed/permeabilized with FoxP3/Transcription Factor staining buffer set (eBioscience) per the manufacturer's instruction. Permeabilized cells were then intracellularly stained with α -FoxP3 antibody. Fluorescent positivity was determined by utilizing appropriate antibody isotype controls. Vaccine DC were also phenotyped for cell surface molecules not involved in cell product release by flow cytometry using the following fluorescently labeled Abs: α -CD266-APC (BioLegend), α -CTLA4-BV786 (BD Biosciences), α -Gal-9-PE (BD Biosciences), α -ICOSL-BV421 (BD Biosciences), α -OX40L-PE (BioLegend), α -PD-L1-BV421 (BioLegend), α -PD-L2-BV711 (BD Biosciences) and appropriate isotype-matched control Abs (BioLegend). Live cell gating was established using Zombie Aqua Viability Dye (BioLegend).

Serum Testing

Baseline and on-treatment (week 5) patient serum specimens were analyzed using a commercial ELISA specific for human CXCL10/IP-10 (R&D Systems) by the IMCPL. The IMCPL also analyzed patient sera for levels of soluble checkpoint molecules using the multiplex Luminex Immuno-Oncology Checkpoint Marker Panel detecting soluble forms of BTLA, CD27, CD28, CD80, CTLA-4, GITR, HVEM, IDO, LAG-3, PD-1, PD-L1, PD-L2, TIM-3 and 4-1BB. In these assays, sera from 19 healthy male and female donors (age range 23-65) were included as normal controls.

RNA Isolation and Gene Expression Analyses

Total RNA was isolated from vaccine α DC1, tumor biopsies and peripheral blood mononuclear cells and subjected to qRT-PCR and GeneChip™ Human Genome U133A 2.0 Arrays (Thermo Fisher Scientific) profiling performed by the University of Pittsburgh Genomics Research Core, to the Oncomine TCRB-LR Assay and to the Oncomine™ Immune Response Research Assay (OIRRA; Thermo Fisher Scientific, Carlsbad, CA) under an institutional material transfer agreement (MTA). TCR β chain repertoire libraries were constructed by multiplex PCR utilizing FR1 and constant gene targeting primers via the Oncomine TCRB-LR assay, then sequenced using the Ion Torrent S5 to a target depth of 1.5M raw reads per library. To evaluate T cell receptor convergence, we searched for instances where TCR β chains were identical in amino acid space but had distinct nucleotide sequences owing to N-addition and exonucleotide chewback within the V-D and D-J junctions of the complementary determining region 3 (CDR3). Targeted gene expression profiling of pre- and post-treatment tumor biopsies was performed via the Oncomine Immune Response Research Assay (OIRRA) using total RNA input.

Biostatistics and Bioinformatics Analyses

All correlative data analyses were conducted using R (version 3.4.3) and Bioconductor. Efficacy and safety were assessed in all patients who received one or more cycles of vaccine +/- dasatinib. The association between variables and response was examined by comparison between responders and non-responders with the two-sided two-sample *t* test, Wilcoxon signed rank or Fisher's exact test, when appropriate. Survival data were analyzed with the Kaplan-Meier method and compared with log-rank tests. For exploratory endpoint survival analyses, the R packages survminer (v 0.2.4) and survival (v 2.11-4) were used. Association of variable with survival endpoints was examined with the Cox proportional hazards model. Comparisons between datasets were performed using non-parametric tests, as detailed in the figure legends. A p-value of 0.05 or less was considered statistically significant. No adjustments for multiple comparisons were performed. Kaplan-Meier analysis was used to estimate the median OS and PFS. Log rank tests were used to compare the OS and PFS between different study arms. Serum cytokines with detection rate < 50% were dichotomized, and those with \geq 50% detection rate were treated as continuous endpoints. Associations of DC cell surface markers and secretion levels of IL-12p70 and IL-10 with vaccine antigen response was determined by performing a student's t-test of the expression level for patients who were vaccine antigen responders against those who were non-responders. Flow cytometry analyses of vaccine α DC1 and patient peripheral blood MDSC and Treg cells were processed to compare absolute and percentage cell counts at baseline. Change between time points was determined by calculating both the difference and fold change between the events, with statistical differences assessed using a student's t-test. Serum levels were determined by ELISA or Luminex for CXCL10 and soluble checkpoint proteins, respectively, at baseline vs. 5 weeks on-treatment. Change between time points was determined by calculating both the difference and fold change between the time points. Statistical testing was performed using student's t-test. Spearman's correlation coefficients were calculated to determine associations present between differentially expressed genes (DEG) in patient mDCs and tumor biopsy tissues and patient immune/clinical responses to treatment. **Gene set enrichment was performed on transcriptional data sets from patient DC and tumor (baseline and on-treatment) samples using the GSEA software (V.4.1.0), a joint project of the University of California-San Diego and the Broad Institute^{S5,S6}.**

Supplemental References Cited:

- S1. Mailliard RB, Wankowicz-Kalinska A, Cai Q, et al. alpha-type-1 polarized dendritic cells: a novel immunization tool with optimized CTL-inducing activity. *Cancer Res.* 2004;64:5934-7.

- S2. Zhao X, Bose A, Komita H, et al. Vaccines targeting tumor blood vessel antigens promote CD8+ T cell-dependent tumor eradication or dormancy in HLA-A2 transgenic mice. *J Immunol.* 2012;188:1782-1788.
- S3. Zhao X, Bose A, Komita H, et al. Intratumoral IL-12 gene therapy results in the crosspriming of Tc1 cells reactive against tumor-associated stromal antigens. *Mol Ther.* 2011;19:805-14.
- S4. Kawakami Y, Dang N, Wang X, et al. Recognition of shared melanoma antigens in association with major HLA-A alleles by tumor infiltrating T lymphocytes from 123 patients with melanoma. *J Immunother.* 2000;23:17-27.
- S5. Subramanian A, Tamayo P, Mootha VK, et al. Gene set enrichment analysis: a knowledge-based approach for interpreting genome-wide expression profiles. *Proc Natl Acad Sci USA.* 2005;102:15545-50. 10.1073/pnas.0506580102.
- S6. Mootha VK, Lindgren CM, Eriksson KF, et al. PGC-1alpha-responsive genes involved in oxidative phosphorylation are coordinately downregulated in human diabetes. *Nat Genet.* 2003;34:267-73. 10.1038/ng1180.